Title
Neurological Impairments in Mice Subjected to Irradiation and Chemotherapy

Journal
Radiation Research, 193(5)

ISSN
0033-7587

Authors
Dey, Deblina
Parihar, Vipan K
Szabo, Gergely G
et al.

Publication Date
2020-05-01

DOI
10.1667/rr15540.1

Peer reviewed

HHS Public Access

Author manuscript

Radiat Res. Author manuscript; available in PMC 2021 May 01.

Published in final edited form as:

Radiat Res. 2020 May ; 193(5): 407–424. doi:10.1667/RR15540.1.

Neurological Impairments in Mice Subjected to Irradiation and Chemotherapy

Deblina Dey[a], **Vipan K. Parihar**[a], **Gergely G. Szabo**[c], **Peter M. Klein**[c], **Jenny Tran**[a], **Jonathan Moayyad**[a], **Faizy Ahmed**[b], **Quynh-Anh Nguyen**[c], **Alexandria Murry**[a], **David Merriott**[a], **Brandon Nguyen**[a], **Jodi Goldman**[a], **Maria C. Angulo**[a], **Daniele Piomelli**[b], **Ivan Soltesz**[d], **Janet E. Baulch**[a], **Charles L. Limoli**[a,1]

[a]Department of Radiation Oncology, University of California, Irvine, California 92697

[b]Department of Anatomy and Neurobiology, University of California, Irvine, California 92697

[c]Department of Neurosurgery, Stanford University, Palo Alto, California 94305

[d]Department of Neurology and Neurological Sciences, Stanford University, Palo Alto, California 94305

Abstract

Radiotherapy, surgery and the chemotherapeutic agent temozolomide (TMZ) are frontline treatments for glioblastoma multiforme (GBM). However beneficial, GBM treatments nevertheless cause anxiety or depression in nearly 50% of patients. To further understand the basis of these neurological complications, we investigated the effects of combined radiotherapy and TMZ chemotherapy (combined treatment) on neurological impairments using a mouse model. Five weeks after combined treatment, mice displayed anxiety-like behaviors, and at 15 weeks both anxiety- and depression-like behaviors were observed. Relevant to the known roles of the serotonin axis in mood disorders, we found that 5HT1A serotonin receptor levels were decreased by ~50% in the hippocampus at both early and late time points, and a 37% decrease in serotonin levels was observed at 15 weeks postirradiation. Furthermore, chronic treatment with the selective serotonin reuptake inhibitor fluoxetine was sufficient for reversing combined treatment-induced depression-like behaviors. Combined treatment also elicited a transient early increase in activated microglia in the hippocampus, suggesting therapy-induced neuroinflammation that subsided by 15 weeks. Together, the results of this study suggest that interventions targeting the serotonin axis may help ameliorate certain neurological side effects associated with the clinical management of GBM to improve the overall quality of life for cancer patients.

INTRODUCTION

Clinical radiation therapy for primary and secondary central nervous system (CNS) malignancies can induce a wide spectrum of learning and memory deficits, adversely affecting spatial, temporal and working memory (1, 2). Many of these debilitating impairments are progressive and persistent, and show little to no decrease over the remaining

[1]Address for correspondence: Department of Radiation Oncology, University of California Irvine, Medical Sciences I, Room B-146B, Irvine CA 92697-2695; climoli@uci.edu.

lifetime of patients. In addition, a significant number of brain tumor patients develop mood disorders that further compromise quality of life (3). Glioblastoma multiforme (GBM) is the most aggressive primary brain tumor. Temozolomide (TMZ) is currently used as a first-line concurrent and adjuvant chemotherapeutic agent, increasing both overall and progression-free survival in GBM patients (4). Furthermore, GBM patients typically receive whole-brain fractionated X-ray irradiation to a total dose of 60 Gy delivered in 2 Gy fractions over 6 weeks (5, 6). Such clinically relevant radiation exposures have clearly been shown to induce cognitive impairments (1, 2); treatment using radiotherapy and TMZ (combined treatment) has similarly been shown to elicit significant adverse neurocognitive side effects (4, 6). Although long-term survivors of GBM suffer from depression (7) and anxiety (8, 9), few studies have been done to systematically analyze the effect of combined treatment on mood (10,11). Given the number of cancer patients suffering from mood disorders (3), it is crucial to investigate the effects of combined treatment on anxiety and depression, and to identify the underlying molecular mechanisms that are disrupted as a result of the combined treatment paradigm.

The neuropathologies underlying mood disorders are not well understood; however, in humans the regions of the brain most commonly observed to be dysregulated in such disorders include the prefrontal and subgenual cingulate cortex, thought to be involved in emotional experience and processing, and the subcortical hippocampus and amygdala, which are involved in emotional memory formation and memory retrieval (12). Therapies involving vagus nerve stimulation have shown some efficacy and are thought to alter levels of serotonin, norepinephrine, GABA and glutamate, correcting dysfunctional neurotransmitter modulatory circuits in the brains of patients with depression (12). Dysfunction in serotonergic neurotransmission is closely associated with major depressive disorders (13), whereby reduced 1-tryptophan synthesis, altered release or reuptake of serotonin (5-HT) or disruption of postsynaptic 5-HT receptors, can lead to depression (14, 15). Similarly, depletion of presynaptic stores of 5-HT by reserpine elicits depression-like syndromes both in animals and in humans (16, 17). Conversely, increased concentrations of 5-HT in the brains of patients treated with the monoamine oxidase inhibitor iproniazid experience euphoria and hyperactive behaviors (17). Hippocampal deficits in the G protein-coupled 5HT1A receptor (5HT1AR) are also associated with depression in patients (15) and in animal models of chronic, stress-induced psychiatric disorders (18, 19). The most commonly prescribed antidepressant is the selective serotonin reuptake inhibitor (SSRI) fluoxetine (FLX), widely known under the brand name Prozac® (20, 21). FLX enhances serotonergic neurotransmission in the CNS by inhibiting 5-HT reuptake. Microdialysis studies of rats have shown that acute administration of FLX increases the 5-HT content in the dialysate in both the raphe nucleus (22) and striatum of the brain (23), and that chronic administration of FLX promotes increased hippocampal neurogenesis (24).

In the current study, the emotional and cognitive effects of combined treatment in mice, at early and late times (5 and 15 weeks, respectively) postirradiation, were evaluated in the absence of confounding underlying disease (i.e., GBM) and with an emphasis on the serotonin axis within the hippocampus (Fig. 1A). The outcome of these experiments suggests that combined treatment elicited anxiety- and depression-like behavior, and impaired learning and memory. Furthermore, the data indicated that combined treatment

elicits decreased expression of 5HT1AR at both early and late times after treatment and decreased 5-HT levels at 15 weeks postirradiation. However, treatment with the SSRI FLX reversed combined treatment-induced depressive-like behavior at 15 weeks postirradiation in mice. Previously reported studies from our laboratory have indicated that cranial irradiation or systemic chemotherapy results in elevated neuroinflammation (25, 26). Similarly, our current study revealed increased microglial activation in the CA1 and CA3 regions of the hippocampus 5 weeks postirradiation, which subsided 10 weeks later, suggesting transient combined treatment-induced neuroinflammation. Together, these new data implicate impaired serotonin signaling in the mouse brain receiving combined treatment, as a factor contributing to early and persistent neurocognitive deficits observed after combined irradiation and TMZ treatment.

MATERIALS AND METHODS

Animals and Combined Radiation and TMZ Treatment

All animal procedures described in this study were in accordance with NIH guidelines and approved by the University of California Irvine and Stanford University Institutional Animal Care and Use Committees. Unique cohorts used for the 5- and 15-week studies were divided into two experimental groups (control and combined treatment). Each cohort consisted of 6-month-old wild-type male mice (C57BL/6J, JAX), housed in groups of 2–4 mice per individually-ventilated cage and maintained in standard housing conditions (20°C ± 1°C; 70% ± 10% humidity; 12:12 h light-dark schedule) and provided *ad libitum* access to food (Envigo Teklad 2020x, Indianapolis, IN) and water.

Animals were randomized between experimental groups without any pre-selection criteria. For cranial irradiation, isoflurane-anesthetized mice were placed in an X-RAD 320 irradiator (Precision X-ray Inc, North Branford, CT) without restraint. Mice were positioned under a collimated (1.0 cm^2 diameter) beam for head-only irradiation, such that the cerebellum, eyes and rest of the body were shielded from exposure to radiation. The irradiator was equipped with a hardening filter to eliminate low-energy X rays and minimize skin damage. X-ray irradiation was delivered at a dose rate of 1.10 Gy/min. Mice received three fractionated X-ray doses on alternating days (8.67 Gy each day) for a total dose of 26 Gy. Mice received three concomitant doses of TMZ (25 mg/kg, in 1% ethanol) via intraperitoneal (i.p.) injection in the first week, alternating with fractionated irradiation. For the subsequent three weeks, mice received nine additional adjuvant TMZ (67 mg/kg i.p.). TMZ dosing was based on human studies using a concomitant dose of 75 mg/m^2 and an adjuvant dose of 200 mg/m^2. TMZ doses were calculated for mice using the human equivalent dose formula reported elsewhere (27). Altogether, the above-described treatment paradigm is referred to as combined treatment and is reflective of the Stupp protocol, which is currently in use in clinical cancer treatments (6). Control mice were sham irradiated and received vehicle injections on the same schedule as the mice receiving combined treatment.

Follow-up studies consisted of additional cohorts of animals. The first cohort included three groups of mice that received 26 Gy irradiation alone (plus vehicle injections), 12 doses of TMZ alone or vehicle injections (1% ethanol solution) for comparison to combined treatment. The second cohort included three groups that received combined treatment,

combined treatment with FLX (25 mg/kg/day) or vehicle to evaluate the efficacy of FLX to reverse combined treatment-induced depression. FLX-HCl (Selleckchem, Houston, TX) was administered during weeks 6–15 in the drinking water, starting one week after the final TMZ injection. FLX solutions were protected from light in opaque water bottles that were replaced every 3 days (28–30).

The body weights of all mice were recorded prior to receiving drug injections in week 1 through week 4. In the five-week study, the mean weight of control mice was 33.5 ± 0.66 g at week 1 and 34.2 ± 0.74 g at week 4, and the mean weight of mice receiving combined treatment was 33.0 ± 0.55 g at week 1, falling to 27.1 ± 0.53 g by week 15. In the 15-week study, the mean weight of control mice was 31.2 ± 0.47 g at week 1 and 31.9 ± 0.40 g at week 4, and the mean weight of mice receiving combined treatment was 32 ± 0.47 g at week 1, falling to 29.8 ± 0.38 g by week 4.

Behavioral Testing

All behavioral tests were performed during the light period of the day in the vivarium light:dark cycle. Data were collected and analyses performed by independent observers who were blinded to the animal treatment groups.

Open field test (OFT) for anxiety-like behavior.—In the OFT, the more time the rodent spends hugging the walls of the arena, the more anxious it is thought to be, while exploring the center of the arena is a measure of exploration or boldness.(31). The open field was comprised of a well-lit (915 lux) acrylic box (30 × 30 × 30 cm). Mice were placed in the center of the box and allowed to explore for 5 min (31). The total distance traveled by each mouse and the total time spent in the central zone (15 × 15 cm) of the box were analyzed using EthoVision® XT version 8.5 software (Noldus Information Technology, Sterling, VA). Less time spent in the central area of the box demonstrates anxiety-like behavior in the mouse (31). At the end of 5 min, each animal was removed and the arena was thoroughly cleaned with ethanol.

Elevated plus maze (EPM) test for anxiety-like behavior.—The EPM was comprised of an acrylic surface with four elevated arms (75 cm above the floor, 110 cm long and 10 cm arm width) with two opposing arms enclosed with 42-cm high walls (i.e., closed arms). The maze was subdivided into five different zones: two open arm zones, two closed arm zones and a central zone (10 × 10 cm) where the arms intersect. The light intensity at the open arms of the EPM was 915 lux. Mice were initially placed in the central zone of the EPM, with their head facing towards a closed arm. Each mouse was allowed to freely explore the maze for 5 min. The frequency of entries and the amount of time spent in each arm was video recorded. Entry into a zone was defined as all four paws of the mouse crossing into a new zone. At the end of 5 min, each mouse was removed from the EPM and placed back in its home cage. The EPM apparatus was thoroughly cleaned between each trial to prevent any influence of odor-related cues from the previous animal.

Light-dark box (LDB) exploration test.—The LDB exploration test assesses anxiety in rodents. The light-dark test utilized an arena (45 × 30 × 27 cm) where one third of the box

was a dark compartment and the other two thirds was a well-lit compartment. The light and dark compartment were connected via a small opening (7.5 × 7.5 cm) that allowed the mice to freely move between the light and dark compartments. The light intensity measured in the light chamber was 900 lux and 4 lux in the dark chamber. Mice were placed at the center of the light compartment facing opposite to the small opening. The number of transitions between the compartments and the total time spent in the light compartment was recorded to quantify performance in this 10-min test. Entry into a chamber was defined as all four paws crossing into the chamber.

Forced swim test (FST) for depression-like behavior.—The FST involved placing a mouse inside a cylinder filled with water, after which the mobility of the animal was measured for 5 min. Increased time spent immobile and floating indicates depression-like behavior (32). The apparatus for the FST was a glass beaker (inner diameter of 15 cm, depth of 20 cm) filled with tap water (20–22°C) to a depth of 16 cm. The depth of water used ensured that the animal could not touch the bottom of the container with their hind paws or their tail. Mice were placed in the FST apparatus for a single video-recorded session lasting 5 min. Data were collected on the immobility or swimming behavior of the mouse by two independent observers who were blinded to the animal groups. The light intensity was 915 lux. Swimming in the FST was defined as the horizontal movement of the animal in the swim chamber or vertically directed movement with forepaws mostly above the water along the wall of the swim chamber. However, immobility or floating was defined as the minimum movement necessary to keep the head above the water level. Mice were removed from the water at the end of 5 min and gently dried and placed back in their home cages. The total immobility time spent over the trial duration was calculated for every mouse and was used to quantify depression-like behavior (32).

Morris water maze (MWM) test.—The MWM test was used to study the effect of combined radiation and TMZ treatment on spatial memory. The MWM was comprised of a circular pool (121.9 cm diameter, 72 cm high) filled with water to a depth of 52 cm to prevent mice from escaping the tank. There was a hidden platform (11.43 cm diameter) 2 cm below the water surface. The four geometrical cues that surround the maze provide for spatial learning and navigation with respect to the submerged platform. To conceal the platform, the water was made opaque using nontoxic white paint. During an initial training period, mice participated in three trials per day for six consecutive days. Rodents were placed in different quadrants of the tank in a random sequence and then allowed to swim until they found the slightly submerged platform. The platform was in the same quadrant of the tank throughout the test period. Task completion was defined as successfully finding and staying on the platform for at least 2 s. Mice were then allowed to remain on the platform for 10 s to reinforce the platform quadrant location before being returned to their home cage. Mice unable to locate the platform within 60 s were assisted to the platform where they were allowed to remain for 10 s and were assigned a maximum time of 60 s. To test memory retrieval, on day 7 a probe trial was performed where the platform was removed. Mice were placed in one quadrant and allowed to swim for 60 s and the times spent swimming in each quadrant were analyzed. Data were analyzed using EthoVision XT version 8.5 software. The light intensity at the surface of the water was 16 lux.

Electrophysiology

At 4 months postirradiation and TMZ treatment, mice were deeply anesthetized and rapidly decapitated. Brains were immediately immersed in ice-cold cutting solution containing (in m*M*): 85 NaCl, 75 sucrose, 25 glucose, 24 $NaHCO_3$, 4 $MgCl_2$, 2.5 KCl, 1.25 NaH_2PO_4 and 0.5 $CaCl_2$. Coronal slices (300 μm) containing the hippocampus were prepared using a vibratome (Leica Biosystems, Nussloch, Germany). Brain slices were then incubated in 35°C cutting solution for 1 h. Prior to recording, brain slices were transferred to artificial cerebrospinal fluid (aCSF) consisting of (in m*M*): 126 NaCl, 26 $NaHCO_3$, 10 glucose, 2.5 KCl, 2 $MgCl_2$, 2 $CaCl_2$, 1.25 NH_2PO_4. All solutions were equilibrated with 95% O_2/5% CO_2.

Intracellular recordings were performed in a submerged chamber perfused with oxygenated aCSF at 2.5 ml/min and maintained at 33°C by a chamber heater (BadController V, Luigs & Neumann Feinmechanik und Elektrotechnik GmbH). Hippocampal neurons were visualized using DIC illumination on an Olympus BX61WI microscope (Olympus Microscopy, Tokyo, Japan) with a CCD camera (Hamamatsu Photonics, Bridgewater, NJ). Recording pipettes were pulled from thin-walled borosilicate capillary glass (King Precision Glass Inc., Claremont, CA) using a P97 puller (Sutter Instrument, Novato, CA) and were filled with (in mM): 126 K-gluconate, 10 HEPES, 4 KCl, 4 ATP-Mg, 0.3 GTP-Na, 10 phosphocreatine (pH-adjusted to 7.3 with KOH, osmolarity of 290 mOsm). Pipettes had a 3–5 MΩ tip resistance.

Whole-cell recordings were performed on CA1 superficial layer pyramidal neurons in the ventral hippocampus. Firing properties were assessed during injected current steps (−200 to 750 pA, 1 s). Input resistance was calculated from the change in steady-state membrane potential resulting from hyperpolarizing current injections, while sag was measured as the difference between the steady-state and peak negative potential during a −100 pA hyperpolarizing current injection. sEPSC activity was measured while neurons were held at −65 mV and the decay time constant was calculated as the time required for the average sEPSC recorded from each neuron to return to 63% of baseline levels. Series resistance was compensated at 65% during all sEPSC recordings via Axon™ MultiClamp™ software (Molecular Devices, Sunnyvale, CA).

Data were acquired using the following, all from Molecular Devices: pClamp software with a Multiclamp 700B amplifier, low-pass filtered at 2 kHz, and digitized at 10 kHz (Digidata 1440A). Data analysis was performed using Clampfit (Molecular Devices) and custom-written Python scripts.

Immunohistochemistry

After completion of all behavioral tests, 4 mice from each group were perfused with 4% paraformaldehyde and 30-μm thick coronal sections were prepared using a cryostat. For each end point, 3–4 representative coronal brain sections from each of 4 animals per experimental group were selected at approximately 15-section intervals.

Quantification of CD68-positive Activated Microglia

To visualize activated microglia, 30-pm thick brain sections were washed in phosphate buffered saline (PBS), subjected to peroxide treatment (30%) for 30 min, followed by blocking for 30 min in 2% (wt/vol) goat serum and then incubated with a primary antibody mixture containing 2% goat serum, 0.1% Triton™ X-100 and rat antimouse CD68 (1:500; AbD Serotec/Bio-Rad, Raleigh, NC) for 24 h. Sections were then treated for 1 h with biotinylated rabbit anti-rat antibody (1:500; Vector® Laboratories, Burlingame, CA), rinsed thoroughly in PBS, treated in VECTASTAIN® ABC kit (Vector Laboratories) for 30 min, processed for color development (Vector Gray, ZE 0419) for 5 min and mounted on gelatin-coated slides. Sections were counterstained with nuclear fast red after 24 h. Unbiased stereology was undertaken to quantify $CD68^+$ cells. Stereologic quantification was conducted using a Nikon Eclipse TiE microscope (Tokyo, Japan) with an MBF CX9000 color digital camera, a 100× oil-immersion (1.30 NA) objective lens, a 3-axis stage and Stereo Investigator software version 9 (MBF Bioscience, Williston, VT). For each animal, $CD68^+$ cells were quantified based on stereological principles, where each measuring frame was 65 × 65 μm, laid on a grid size of 125 × 125 μm to encompass the subregional contour using the optical fractionator workflow. The Gundersen coefficient error, representing the standard error of the mean of repeated estimates divided by the mean, was in the range of 0.05–0.10 for all counts in this study.

Quantification of 5HT1AR Puncta

To visualize serotonin receptor expression, sections from the anterior hippocampus were immunostained for the 5HT1A receptor. Sections were initially washed in PBS (pH 7.4), blocked for 30 min in PBS containing 2% (wt/vol) bovine serum albumin (BSA), then incubated for 24 h in a primary antibody mixture of PBS containing 1% BSA, 0.1% Triton X-100 and rabbit polyclonal 5HT1AR (1:100; reacts with mouse and affinity purified by protein A; Biorbyt LLC, St. Louis, MO). The next day, after PBS washes, sections were incubated for 1 h with a mixture of secondary donkey anti-rabbit IgG tagged with Alexa Fluor® 594 (1:100; Invitrogen™, Carlsbad, CA), rinsed thoroughly in PBS, and then mounted on slides using a slow fade/antifade mounting media (Life Technologies, Carlsbad, CA). Image stacks composed of nine z planes (0.5-μm spacing) were generated using a Nikon Eclipse TE 2000-U microscope. Three 60× images from the stratum radiatum and stratum lacunosum-moleculare layer of CA1 region and two 60× images of the CA3 region from each hippocampus were captured. The receptor number in each image was counted using Imaris software (Bitplane AG, Zurich, Switzerland). Each constituent image comprising the Z-stack had a resolution of 1,024 × 1,024 pixels. To optimize the quantification of immunore-active 5HT1A receptor puncta, confocal Z-stacks were first deconvoluted using AutoQuant X3 software (Media Cybernetics Inc., Rockville, MD) to correct Z-axis distortion. High-resolution images were then exported into Imaris for 3D deconvolution using a predefined diameter threshold (0.5 μm). The density of the 5HT1A receptor labeling was then quantified by conversion to a 3D surface, derived from confocal Z-stacks. Both the spot analysis and minimum surface diameter parameters were manually adjusted to optimize puncta detection and kept constant thereafter for all subsequent analyses (33).

High-Performance Liquid Chromatography (HPLC) Measurement of Serotonin

Sample preparation.—Mice were anesthetized with isoflurane and then decapitated, after which both hippocampi were dissected out and immediately frozen in liquid nitrogen, prior to storage at −80°C. Each hippocampus was weighed and homogenized in a 20× volume of homogenizing buffer on ice. The homogenizing buffer consisted of a 1:1 solution of acetonitrile and methanol. Brain samples were homogenized (Polytron®) for 2 min and then subjected to sonication for 1 min in a Digital Sonifier® Branson Ultrasonics, Dansbury, CT). Samples were centrifuged at 13,000*g* for 15 min and the supernatant was decanted into a glass vial. To maximize recovery of serotonin from samples, each pellet was again homogenized with an additional 100 μl of homogenizing buffer, followed by sonication and centrifugation. The supernatant from both extractions was combined and dried under nitrogen air on ice. The dried samples were reconstituted with 100 μl of homogenization buffer in preparation for injection into an HPLC column.

Standard solutions.—Serotonin hydrochloride (Sigma-Aldrich® LLC, St. Louis, MO was used as a reference standard. The standard stock solutions were prepared by dissolving the compound in a solution of LC-MS grade 1:1 acetonitrile and methanol. A set of serotonin standards was prepared in a range from 10–2,500 pg/5 μl and was run simultaneously with brain-derived samples described above.

Gradient elution.—Chromatographic analysis was performed using a 1.7-μm BEH Amide column, 2.1 × 50 mm (Waters® Corp., Milford, MA) under HILIC conditions. For mobile phase A, 0.1% formic acid in water (LC-MS grade; Honeywell Intl. Inc., Morris Plains, NJ) was used, and for phase B, acetonitrile (LC-MS grade; Honeywell) was used. The injection volume for all standards was 5.0 μl and that of brain extract was 10 μl. The flow rate was 0.4 ml/min. A step gradient elution was performed as follows: starting with 90% B to 3.51 min and at 3.51 min change to 40% B to 5.50 min. Re-equilibration to the original condition was done for 15 min.

Instrumentation

The HPLC system consisted of a 1200 series degasser, binary pump and autosampler (Agilent Technologies, Santa Clara, CA). An Agilent 1290 fluorescent detector was used with 279-nm excitation and 320-nm emission. Both fluorescence excitation and emission spectra were obtained during the runs to further identify the serotonin peaks. Data were acquired and analyzed using Agilent OpenLab CDS with ChemStation.

Statistics

All statistical analyses were performed using either GraphPad Prism data analysis software version 7.03 (LaJolla, CA), or for whole cell recordings, custom-written Python scripts. For analyses of OFT, EPM, LDB, FST, immunohistochemistry data, HPLC measurements of serotonin, the different parameters from control and combined treated groups were assessed using unpaired Mann-Whitney U test. For combined treatment with or without FLX, one-way analysis of variance (ANOVA) was used. Data pertaining to spatial learning in the MWM (i.e., latencies to reach platform and swim speed in successive learning sessions) were analyzed using two-way RM-ANOVA followed by Bonferroni's multiple comparisons

test. Water maze probe tests (i.e., dwell time in platform quadrant and proximity to the platform) were compared using paired Student's *t* tests. For whole cell electrophysiology recordings, all differences between treatment groups were evaluated using two-tailed *t* tests run in Python. Data are expressed as mean ± SEM from a minimum of three independent measurements. $*P < 0.05$, $**P < 0.01$ and $***P < 0.001$. Statistical significance was assigned at $P < 0.05$.

RESULTS

Combined Treatment Elicits Anxiety and Depression-like Behaviors

Five or 15 weeks after final irradiation, mice receiving combined treatment or concurrent control treatment were tested for anxiety-like behavior using open-field testing (OFT), the elevated plus maze (EPM) and light-dark box exploration (LDB) (Fig. 1A). The OFT is used for measuring exploratory behavior in a novel arena, providing an indication of fear or anxiety-like tendencies, whereby mice with less anxiety explore over greater distances and spend more time in the central part of the open field (31). As such, we tracked each mouse as it freely explored an arena for 5 min (Fig. 1B–E). At 5 weeks postirradiation, mice receiving combined treatment traveled a shorter total distance than control animals and also spent less time in the center of the field, suggesting a combined treatment-induced anxiety phenotype (Fig. 1B and C, $P = 0.003$ and $P = 0.02$, respectively). This behavior was similarly observed at 15 weeks postirradiation (Fig. 1D and E, $P = 0.0004$ and $P = 0.05$, respectively), indicating persistence of this combined treatment-related anxiety-like behavior.

To further assess anxiety-like behavior after combined treatment, mice were evaluated on the EPM (Fig. 2A and B). In this test, animals with increased anxiety spend more time in the closed arms than in the open arms of the maze and will enter the open arms less frequently (34). At 5 weeks postirradiation, both the combined treatment and control mice spent an equivalent amount of time in the open arms; however, the mice that received combined treatment showed subtle signs of anxiety-like behavior by avoiding entry into the open arms (Fig. 2A, $P = 0.3$ and $P = 0.04$, respectively). At 15 weeks postirradiation, mice receiving combined treatment displayed anxiety-like behavior by spending less time than control mice in the open arms (Fig. 2B, $P = 0.002$). Interestingly, the mice that received combined treatment also displayed some characteristics of decreased anxiety, with an increased preference for entering the open arms of the maze at 15 weeks postirradiation compared to the control mice (Fig. 2B, $P = 0.009$). While somewhat discordant, the results of the EPM at 15 weeks postirradiation consistently demonstrated that combined treatment induced elements of anxiety-like behavior compared to control mice.

As a third measure of anxiety-like behavior, mice were also subjected to the LDB exploration test (Fig. 2C and D). As with the EPM, animals exhibiting anxiety-like behavior are less willing to spend time in the bright chamber and transition less frequently between the light and dark chambers than normal control mice. At 5 weeks postirradiation, mice receiving combined treatment showed no significant preference for either compartment, (Fig. 2C, $P = 0.2$), but did make significantly fewer transitions between the light and dark compartments (Fig. 2C, $P = 0.007$). These data again suggest that combined treatment may

elicit increased anxiety-like behavior at early times after treatment. Similarly, while mice that received combined treatment showed no significant aversion to the light compartment at 15 weeks postirradiation compared to concurrent controls (Fig. 2D, $P = 0.4$), they also made fewer transitions between the light and dark compartments (Fig. 2D, $P = 0.04$). Together, open field, elevated plus maze and light-dark box exploration tests suggest that mice receiving combined treatment may exhibit some induced anxiety-like behavior at early times after treatment, which are persistent and may become more pronounced at later times after treatment.

Because depression is a common side effect of combined radiation and TMZ treatment in patients, the mice receiving combined treatment and the concurrent control mice were also tested for depression-like behavior using the forced swim test (FST) (Fig. 2E). At 5 weeks postirradiation, no depression-like changes were observed in the time in which the combined treatment group spent floating compared to control animals (Fig. 2E, $P = 0.6$); however, at 15 weeks after combined treatment, the treated mice displayed significant depression-like behavior, spending much more time floating, compared to the control mice (Fig. 2E, $P = 0.009$). Thus, these findings suggest that the combination of X rays and TMZ might elicit delayed onset of depressionlike behavior in mice.

Individual Irradiation or TMZ does not Induce Anxiety

To emphasize the effect of combined treatment on anxiety- or depression-like behaviors, independent cohorts of mice that received 26 Gy fractionated irradiation alone or TMZ treatment alone compared to concurrent controls were also tested for impairments at 15 weeks after treatment using the same battery of behavior tests employed to evaluate the effects of combined treatment (Fig. 3). The OFT demonstrated that neither the irradiated nor the TMZ-treated mice exhibited reductions in total distance traveled or time spent in the center relative to concurrent control mice [Fig. 3D, $F(2,30) = 2.55$, $P = 0.1$; and Fig. 3E, $F(2,30) = 2.00$, $P = 0.2$, respectively], distinctly in contrast to the findings at 15 weeks after combined treatment. Similarly, mice administered 26 Gy irradiation or TMZ alone spent the same percentage of time in the open arms of the EPM, unlike the mice that received combined treatment (Fig. 2B), and made the same percentage of entries into the open arms at 15 weeks after treatment as the controls [Fig. 3F, $F(2,30)=0.70$, $P = 0.5$; and Fig. 3G, $F(2,30)=0.27$, $P = 0.8$, respectively]. Furthermore, while mice that received combined treatment made fewer transitions between the light and dark chambers in the LDB (Fig. 2D), the mice that received either 26 Gy irradiation or TMZ treatment alone spent similar amounts of time in the light compartment compared to each other and to the control mice, and had similar numbers of transitions between the light and dark compartments, also compared to each other and to controls [Fig. 3H, $F(2,29) = 0.15$, $P = 0.9$; and Fig. 3I, $F(2,29) = 1.44$, $P = 0.3$, respectively]. These data suggest that combined treatment is more likely to induce anxiety-like behavior than either fractionated cranial radiotherapy or chemotherapy alone. However, similar to the mice receiving combined treatment (Fig. 2E), the 26 Gy fractionated radiation alone was capable of inducing depression-like behavior at 15 weeks postirradiation, whereby the mice displayed increased immobility compared to controls (Fig. 3J, $P = 0.006$). Mice treated with TMZ alone performed in a manner similar to control animals [$P = 0.5$, $F(2,27) = 5.24$, $P = 0.01$].

Cognitive Performance is Persistently Disrupted in Mice that Received Combined Treatment

In patients, radiotherapy for CNS malignacies is known to induce a variety of learning and memory deficits (1, 2). Therefore, the Morris water maze (MWM) test was utilized to evaluate spatial learning and memory in mice that received combined treatment, at 15 weeks postirradiation (Fig. 4). While the swim velocity of both the combined treatment and control groups decreased across training days 1–6 [$F(5,100) = 19.09$, $P < 0.0001$], there was no difference in velocity between the two groups on any given training day [Fig. 4A; $F(1,20) = 1.33$, $P = 0.3$]. As the mice learned the water maze task, both treatment groups showed progressive decreases in their latency to reach the hidden platform across training days [$F(5,100) = 17.56$, $P < 0.0001$] and likewise, both groups exhibited similar latencies to reach the platform [Fig. 4B; $F(1,20) = 2.47$, $P = 0.1$].

In a probe trial performed 24 h after the final training session (day 6), two-way ANOVA demonstrated no quadrant effect [$F(3, 60) = 2.39$, $P = 0.08$] and no significant group X quadrant interaction [$F(3, 60) = 0.66$, $P = 0.6$]. However, significant differences within the control group were found in the times spent between the platform quadrant and the right or opposite quadrants, indicating intact memory retrieval from the six days of training (Fig. 4C; $P = 0.05$, paired Student's t test). Conversely, mice that received combined treatment demonstrated impaired memory retrieval when searching for the previously learned platform location, exhibiting almost equal affinity for all four quadrants (Fig. 4D; $P > 0.05$, paired Student's t test). Further analysis evaluating the number of crossings and time spent within the platform zone indicated no differences between the combined treatment and control groups (Fig. 4E and F).

Combined Treatment Does Not Alter the Electrophysiological Properties of CA1 Pyramidal Neurons

Since many of the cognitive deficits induced by radiation and chemotherapy have been linked to hippocampal impairments (33), electrophysiological properties of CA1 pyramidal neurons were determined after completion of behavior testing for the 15-week postirradiation mice. The employed paired cell recordings represent a highly sophisticated and sensitive method of evaluating synaptic connections. Because the behavioral data indicated that combined treatment produces greater disruptions in anxiety and depression-like behaviors than disruptions in learning and memory performance, the ventral portion of the hippocampus was targeted for electrophysiological analysis. While the dorsal hippocampus has a more prominent role in spatial learning tasks (35), signaling from the ventral hippocampus is important in the regulation of anxiety and depression behavior (36–38).

No discernable changes were observed in the electrophysiological properties of CA1 superficial layer pyramidal neurons in the ventral hippocampus after combined treatment (Fig. 5). The resting membrane potential of neurons in both treatment groups remained equivalent during whole-cell recordings (Fig. 5A; control: -66.7 ± 0.4 mV, n = 16 cells; combined treatment: -66.3 ± 0.4 mV, n = 25 cells; $P = 0.5$). Furthermore, CA1 pyramidal neurons from control mice and those receiving combined treatment were subjected to a

range of brief current injections to test for changes in cell-intrinsic properties (Fig. 5B). Combined treatment neither altered the input resistance of CA1 pyramidal neurons (Fig. 5C; control: 107 ± 6.3 MΩ, n = 16 cells; combined treatment: 100 ± 5.2 MΩ, n = 25 cells; P = 0.4), nor the amplitude of the hyperpolarization sag when neurons were injected with a −100 pA current (Fig. 5D; control: 1.7 ± 0.20 mV, n = 16 cells; combined treatment: 1.7 ± 0.12 mV, n = 25 cells; P = 0.9). Additionally, the excitability of CA1 pyramidal neurons was not altered in mice that received combined treatment, with the same rheobase current-evoking action potentials in both treatment groups (Fig. 5B and E; control: 122 ± 16.4 pA, n = 16 cells; combined treatment: 120 ± 5.8 pA, n = 25 cells; P = 0.9).

The spontaneous, excitatory, postsynaptic activity received by CA1 pyramidal neurons was also unaltered by combined treatment (Fig. 5F). CA1 pyramidal neuron spontaneous excitatory postsynaptic current (sEPSC) frequency remained at similar levels in control (2.4 ± 0.42 Hz, n = 16 cells) and animals receiving combined treatment (Fig. 5G; 2.6 ± 0.30 Hz, n = 25 cells; P = 0.7). To examine differences in the sEPSC properties within individual neurons, all sEPSCs detected within a 200-s recording period from that cell were averaged together to generate a standard profile (Fig. 5H). Neither the amplitude of sEPSCs (Fig. 5I, control: 13.4 ± 0.86 pA, n = 16 cells; combined treatment: 13.9 ± 0.73 pA, n = 25 cells; P = 0.67), nor the rate at which sEPSCs decay (Fig. 4J; control: 7.5 ± 0.37 ms, n = 16 cells; combined treatment: 7.7 ± 0.33 ms, n = 25 cells; P = 0.7) was altered by combined treatment. Thus, combined treatment did not appear to affect excitatory network activity within the hippocampus of mice in the 15-week postirradiation study.

Microglial Activation is Acutely Elevated by Combined Treatment

Microglia are the primary immune cells of the CNS, responding to injury or disease by removing damage-related debris from the brain and serving a neuroprotective function. However, persistent microglial activation is a hallmark of increased inflammation and is one of the detrimental side effects linked to normal tissue injury after clinically relevant radiation or chemotherapy treatments (25, 26). Therefore, the number of $CD68^+$ activated microglia was quantified for mice receiving combined treatment and control mice (Fig. 6). At 5 weeks postirradiation, stereology counting revealed a doubling in the number of activated microglia in the CA1 (Fig. 6A, B and E) and CA3 (Fig. 6C, D and F) hippocampal regions of mice receiving combined treatment compared to their concurrent controls (Fig. 6E and F; P > 0.05). However, by 15 weeks postirradiation the number of $CD68^+$ microglia in the CA1 and CA3 of the combined treatment mouse brain had returned to levels similar to that of controls (Fig. 6G and H; P = 0.4 and P = 1.0, respectively).

Combined Treatment Induces a Delayed Decrease in Hippocampal Serotonin Signaling Pathways

The serotonergic system plays a significant role in the etiology of anxiety and depression, with either a knockout or blockade of the 5HT1A receptor leading to increasing anxiety-like behavior in mice (39). Given these observations, immunohistochemical analyses were performed to investigate whether combined treatment induced changes in hippocampal 5HT1AR levels. The literature has shown the anatomical distribution of 5HT1AR to be in the stratum oriens (SO), radiatum (SR) and lacunosum moleculare (SLM) layers of the CA1

and CA3 hippocampal subfields, with 5HT1AR mRNA localized in the pyramidal cell layer of the CA1 and CA3 subfields (40). 5HT1AR protein is also expressed in pyramidal cells and interneurons of both the cortex and hippocampus (41, 42). At 5 weeks postirradiation a significant decrease in 5HT1AR puncta was observed in the CA1 region of the hippocampus of mice that received combined treatment compared to controls (Fig. 7A–C, $P = 0.0002$), as well as in the CA3 hippocampal subfield (Fig. 7D–F, $P = 0.0002$). Similarly, at 15 weeks postirradiation, the number of 5HT1AR puncta was reduced in the SR and SLM regions of the CA1 of mice that received combined treatment compared to concurrent controls (Fig. 7G–I, $P = 0.002$), but 5HT1AR puncta had returned to control levels in the CA3 region (Fig. 7J–L, $P = 0.5$).

In addition to changes in 5HT1A receptor protein levels, altered levels of 5-HT in mice receiving combined treatment might contribute to the neurocognitive impairments as well. Therefore, HPLC was performed to measure 5-HT levels in the hippocampus of mice that received combined treatment and controls, whereby all measurements were compared to chromatograms of 5-HT standard solutions (Fig. 8). While hippocampal 5-HT levels were unchanged in the combined treatment group at 5 weeks postirradiation compared to controls (Fig. 8A; 1010 ± 174 pg/mg and 1590 ± 601 pg/mg, respectively; $P = 0.5$), they were significantly reduced in the hippocampus of the combined treatment group at 15 weeks postirradiation (Fig. 8B; 180 ± 14 pg/mg and 286 ± 55 pg/mg, respectively; $P = 0.03$). As with the other findings, individual treatment with 26 Gy fractionated irradiation or TMZ alone was insufficient to alter hippocampal 5-HT levels at 15 weeks *after* treatment (Fig. 8C; 659 ± 81 pg/mg, 624 ± 44 pg/mg and 660 ± 108 pg/mg for control, 26 Gy and TMZ, respectively; [$F(2,12)=0.71$, $P = 0.9$].

Fluoxetine Alleviates Combined Treatment-Induced Depression-like Behavior

Finally, the hypothesis that 5-HT manipulation using the SSRI fluoxetine (FLX) would ameliorate depression-like behavioral deficits observed in mice receiving combined treatment was tested. FLX is a widely used antidepressant that works by inhibiting the reuptake of 5-HT, thus enhancing serotonergic neurotransmission in the CNS. A separate cohort of mice comprised of three groups was used: control, combined treatment and combined treatment with FLX (Fig. 9). One week after the final TMZ dose, the FLX treatment group received FLX (25 mg/kg/day) in their drinking water (28–30) (Fig. 9A). Depression-like behavior was then evaluated among the three groups using the FST. At 15 weeks postirradiation, immobility time varied among the treatment groups [Fig. 9B, $F(2,18) = 4.24$, $P = 0.03$]. As with our first cohort of mice (Fig. 2E) we found that mice receiving combined treatment spent more time immobile than the control mice (Fig. 9B, $P = 0.05$), indicating increased depression-like behavior. However, the mice receiving FLX with combined treatment showed immobility times that were significantly lower than those of mice that received combined treatment alone, and the times were indistinguishable between the FLX-treated mice and the controls, indicating amelioration of depression-like behavior ($P = 0.04$ and $P = 0.8$, respectively).

DISCUSSION

Advancements in the diagnosis and treatment of cancer have led to improvements in local-regional control and progression-free survival for patients with many cancer types, including GBM (43). Even with such encouraging progress, therapy-induced impairments in learning, memory and mood remain a serious unmet concern that is particularly problematic for pediatric cancer survivors and those afflicted with CNS malignancies. Normal tissue toxicities are believed to underlie a majority of the complications associated with the radio- and chemotherapeutic management of cancer. Therefore, sparing neurocognitive functionality is now recognized as a critical criterion for successful therapeutic outcome (44). Importantly, both conformal radiotherapy targeted specifically to the CNS and systemic chemotherapy elicit cognitive dysfunction that exhibits similar pathologies and phenotypic overlap at the cellular level (45). Previously published work from our laboratory has linked both of these cancer therapies to qualitatively similar increases in neuroinflammation and to structural deterioration of mature neurons (33, 34, 46, 47). Furthermore, cranial irradiation elicits persistent oxidative stress in the brain (48, 49). Together, such cellular changes are hypothesized to underlie the learning and memory deficits exhibited in preclinical chemotherapy studies using rodents (50, 51) and observed in patients given cranial radiotherapy (52, 53). In particular, neurological complications are a substantial problem for cancer patients, thereby affecting their quality of life (54, 55). In our current study, we investigated the combined effects of cranial radiotherapy and TMZ treatment (i.e., combined treatment) on neurological function in mice.

The testing of our combined treatment paradigm revealed significant anxiety- and depression-like behaviors. Compared to control mice, animals subjected to combination radio- and chemotherapy showed reluctance to explore stressful environments, indicating a persistent anxiety- and/or depression-like phenotype that emerged between 5 and 15 weeks postirradiation. While data derived from combined treatment cohorts were suggestive of mood disorders, these interpretations may be confounded by resultant hypoactivity. Some divergence between the relative time spent and transitions between compartments was observed in the LDB test, with the latter parameter reaching significance at both 5 and 15 weeks after treatment (Fig. 2C and D). In addition, equivalent swim speeds of control and combined treatment cohorts in the Morris water maze test (Fig. 4A) suggested that measures of anxiety- and depression-like behavior were not confounded by inactivity within the combined treatment group.

Many of the changes reported here with rodents resemble elements of mood disorders that routinely plague cancer survivors (56). While anxiety and depression disorders share some common features (57), they have distinct molecular pathways. Thus, while tricyclic antidepressants can treat depression, benzodiazepines are more commonly used to treat anxiety (58). However, SSRIs have gained in popularity due to their success in treating both anxiety and depression (58). Feelings of uncertainty, lack of confidence, anxiousness and generalized depression are among the mood disorders that persist chronically in cancer patients even long after they have completed their treatment. Longer-term survivors of childhood cancers exhibit many of these same complications, compromising their ability to adapt and integrate into society (59). Behavioral testing in rodents is not without caveats, but

such models provide useful surrogates for dissecting the underlying complications associated with select cancer treatments, while simultaneously avoiding the complications of confounding disease.

Monoamine metabolism and signaling plays a significant role in regulating stress-induced mood disorders (42, 60), and reduced 5-HT neurotransmission has been shown to contribute to depression (61–63). Here, we report for the first time that combined radio- and chemotherapy treatment elicits long-term disruptions in hippocampal serotonergic signaling. Mice with genetic knockdowns of the serotonin receptor 5HT1A are increasingly susceptible to anxiety phenotypes (64). In our study, we found that combined treatment caused marked, acute reductions in 5HT1AR in both the CA1 and CA3 regions of the hippocampus, which persist in the CA1 to at least 15 weeks postirradiation. The differential effects of combined treatment on 5HT1AR expression within CA1 and CA3 at our later time point may be due to the regional sensitivity of different hippocampal subfields to brain insults (65). As baseline 5HT1AR expression is higher in the CA1 than the CA3 (66, 67), any reduction in 5HT1AR induced by our treatment at a later time point may be more dramatic in the CA1 than the CA3. Furthermore, previously published findings demonstrate that CA1 neurons are more susceptible to damage and resultant changes in protein expression in response to insults such as intermittent hypoxia-induced damage as compared to the CA3 (68). Insults like global ischemia, chronic epileptic seizures and oxidative stress have also been shown to cause greater cell death to CA1 neurons than to CA3 pyramidal cells (69, 70). Alternatively, CA1 neurons expressing higher levels of 5HT1AR may be more susceptible to combined treatment-mediated reductions in receptor levels, leading to a more severe effect on CA1 neuron function compared to CA3 neurons. The foregoing possibilities may provide some explanation for reduced 5HT1AR levels in the CA1 versus the CA3 region at 15 weeks postirradiation. Previously published studies that have identified persistent elevations in oxidative stress after irradiation highlight the differential susceptibility of the CNS to oxidative insult (71, 72). Oxidative stress was also elevated in the brains of mice treated with the chemotherapeutic drug Adriamycin (73). Thus, treatment-associated oxidative stress represents a potential biochemical mechanism capable of producing the deficits in serotonergic signaling, and the perturbations in anxiety and depression that we observed. Previously reported studies from our laboratory have demonstrated that even low-dose exposures to charged particle radiation (<1 Gy) are sufficient to cause increased oxidative stress (74).

Serotonergic projections from the raphe nucleus innervate the hippocampus and can affect the excitability and synaptic plasticity of CA1 neurons (75). Thus, serotonergic signaling via 5HT1AR activates inwardly rectifying potassium channels and can hyperpolarize CA1 pyramidal cells (76). 5-HT also modulates fast and slow synaptic inhibition of CA1 principal cells (77). Additionally, 5-HT increases the rectification of CA1 pyramidal cells and sub-threshold EPSP amplitudes (78). Although combined treatment significantly decreases hippocampal 5HT1A receptor expression and decreases 5-HT levels in the hippocampus, we find no changes in electrophysiological properties of the CA1 pyramidal neurons. Currently, the reason for these findings remains uncertain.

Diffuse traumatic brain injury is capable of producing transient neuroinflammation and depression-like behavior (79). Our data demonstrated an acute increase in inflammation within the CA1 and CA3 that diminished by 15 weeks postirradiation. Radiation-induced increases in reactive oxygen species occur rapidly and may persist for weeks to months postirradiation (80), thus leading to increased levels of lipid peroxidation (81, 82). Additionally, increased expression of the proinflammatory cytokines TNFα, IL-1, IL-1β and ICAM-1 occurs in cranially-exposed mice (83). Microglia, as the resident immune cells in the CNS, play an important role in the immunological response within the brain. After a brain injury, microglia become activated and amoeboid in shape (84, 85), a hallmark of neuroinflammation. Moreover, we observed that combined treatment induced activated microglia in the CA1 and CA3, an effect that did not persist at 15 weeks postirradiation. One possible reason for this might involve a gradual decline in proinflammatory cytokines at the later postirradiation time, possibly due to the recovery of the brain from radiation injury, which minimizes persistent inflammatory signatures.

By investigating the ability combined radiation and chemotherapy to induce persistent mood disorders, we identified certain molecular mechanisms associated with the observed aberrant behavioral phenotypes. Early and persistent anxiety-like behavior was observed after combined treatment, along with a decreased number of 5HT1AR serotonin receptors in the CA1 and CA3 hippocampal subfields. Persistent depressive-like behavior in response to combined treatment also correlated with a decrease in serotonin level in the hippocampus. Interestingly, recently published work using similar combined treatment demonstrated benefits of FLX for resolving behavioral dysfunction (10, 11), and our studies, using a more clinically relevant combined treatment paradigm, expand this work further. Here we show that certain neurological impairments of mice given combined treatment involved disruptions to serotonin signaling which might be ameliorated with the SSRI FLX.

ACKNOWLEDGMENTS

We thank Dr. Munjal Acharya, Erich Giedzinski, Ning Ru and Liping Yu for excellent discussions and technical assistance. This work was supported by the National Institute of Neurological Disorders and Stroke (NINDS grant no. R01 NS089575 to CLL).

REFERENCES

1. Meyers CA, Brown PD. Role and relevance of neurocognitive assessment in clinical trials of patients with CNS tumors. J Clin Oncol 2006; 24:1305–09. [PubMed: 16525186]
2. Butler JM, Rapp SR, Shaw EG. Managing the cognitive effects of brain tumor radiation therapy. Curr Treat Options Oncol 2006; 7:517–23. [PubMed: 17032563]
3. Leopold KA, Ahles TA, Walch S, Amdur RJ, Mott LA, Wiegand-Packard L, et al. Prevalence of mood disorders and utility of the PRIME-MD in patients undergoing radiation therapy. Int J Radiat Oncol Biol Phys 1998; 42:1105–12. [PubMed: 9869236]
4. Stupp R, Hegi ME, Mason WP, van den Bent MJ, Taphoorn MJ, Janzer RC, et al. Effects of radiotherapy with concomitant and adjuvant temozolomide versus radiotherapy alone on survival in glioblastoma in a randomised phase III study: 5-year analysis of the EORTC-NCIC trial. Lancet Oncol 2009; 10:459–66. [PubMed: 19269895]
5. Cabrera AR, Kirkpatrick JP, Fiveash JB, Shih HA, Koay EJ, Lutz S, et al. Radiation therapy for glioblastoma: Executive summary of an American Society for Radiation Oncology Evidence-Based Clinical Practice Guideline. Pract Radiat Oncol 2016; 6:217–25. [PubMed: 27211230]

6. Stupp R, Mason WP, van den Bent MJ, Weller M, Fisher B, Taphoorn MJ, et al. Radiotherapy plus concomitant and adjuvant temozolomide for glioblastoma. N Engl J Med 2005; 352:987–96. [PubMed: 15758009]
7. Litofsky NS, Farace E, Anderson F Jr, Meyers CA, Huang W, Laws ER Jr Depression in patients with high-grade glioma: results of the Glioma Outcomes Project. Neurosurgery 2004; 54:358–67. [PubMed: 14744282]
8. Skarstein J, Aass N, Fossa SD, Skovlund E, Dahl AA. Anxiety and depression in cancer patients: relation between the hospital anxiety and depression scale and the European Organization for Research and Treatment of Cancer Core Quality of Life Questionnaire. J Psychosom Res 2000; 49:27–34. [PubMed: 11053601]
9. Arnold SD, Forman LM, Brigidi BD, Carter KE, Schweitzer HA, Quinn HE, et al., Evaluation and characterization of generalized anxiety and depression in patients with primary brain tumors. Neuro Oncol 2008; 10:171–81. [PubMed: 18314416]
10. Gan H, Zhang Q, Zhu B, Wu S, Chai D. Fluoxetine reverses brain radiation and temozolomide-induced anxiety and spatial learning and memory defect in mice. J Neurophysiol 2019; 121:298–305. [PubMed: 30517049]
11. Egeland M, Guinaudie C, Du Preez A, Musaelyan K, Zunszain PA, Fernandes C, et al. Depletion of adult neurogenesis using the chemotherapy drug temozolomide in mice induces behavioural and biological changes relevant to depression. Transl Psychiat 2017; 7.
12. Ressler KJ, Mayberg HS. Targeting abnormal neural circuits in mood and anxiety disorders: from the laboratory to the clinic. Nat Neurosci 2007; 10:1116–24. [PubMed: 17726478]
13. Lucki I The spectrum of behaviors influenced by serotonin. Biol Psychiatry 1998; 44:151–62. [PubMed: 9693387]
14. Cowen PJ, Parrybillings M, Newsholme EA. Decreased plasma tryptophan levels in major depression. J Affect Disord 1989; 16:27–31. [PubMed: 2521647]
15. Moses-Kolko EL, Wisner KL, Price JC, Berga SL, Drevets WC, Hanusa BH, et al. Serotonin 1A receptor reductions in postpartum depression: a positron emission tomography study. Fertil Steril 2008; 89:685–92. [PubMed: 17543959]
16. Butcher LL, Rhodes DL, Yuwiler A. Behavior and biochemical effects of preferentially protecting monoamines in the brain against the action of reserpine. Eur J Pharmacol 1972; 18:204–12. [PubMed: 4537669]
17. Brigitta B Pathophysiology of depression and mechanisms of treatment. Dialogues Clin Neurosci 2002; 4:7–20. [PubMed: 22033824]
18. Wissink S, Meijer O, Pearce D, van Der Burg B, van Der Saag PT. Regulation of the rat serotonin-1A receptor gene by corticosteroids. J Biol Chem 2000; 275, 1321–6. [PubMed: 10625680]
19. Watanabe Y, Sakai RR, McEwen BS, Mendelson S. Stress and antidepressant effects on hippocampal and cortical 5-HT1A and 5-HT2 receptors and transport sites for serotonin. Brain Res 1993; 615:87–94. [PubMed: 8364729]
20. Wong DT, Perry KW, Bymaster FP. Case history: the discovery of fluoxetine hydrochloride (Prozac). Nat Rev Drug Discov 2005; 4:764–74. [PubMed: 16121130]
21. Gram LF. Fluoxetine. New Engl J Med 1994; 331:1354–61. [PubMed: 7935707]
22. Malagie I, Trillat AC, Jacquot C, Gardier AM. Effects of acute fluoxetine on extracellular serotonin levels in the raphe: an in vivo microdialysis study. Eur J Pharmacol 1995; 286:213–7. [PubMed: 8605960]
23. Perry KW, Fuller RW. Effect of fluoxetine on serotonin and dopamine concentration in microdialysis fluid from rat striatum. Life Sci 1992; 50:1683–90. [PubMed: 1375306]
24. Malberg JE, Eisch AJ, Nestler EJ, Duman RS. Chronic antidepressant treatment increases neurogenesis in adult rat hippocampus. J Neurosci 2000; 20:9104–10. [PubMed: 11124987]
25. Acharya MM, Martirosian V, Chmielewski NN, Hanna N, Tran KK, Liao AC, et al. Stem cell transplantation reverses chemotherapy-induced cognitive dysfunction. Cancer Res 2015; 75:676–86. [PubMed: 25687405]
26. Acharya MM, Martirosian V, Christie LA, Riparip L, Strnadel J, Parihar VK, et al. Defining the optimal window for cranial transplantation of human induced pluripotent stem cell-derived cells to

ameliorate radiation-induced cognitive impairment. Stem Cells Transl Med 2015; 4:74–83. [PubMed: 25391646]

27. Reagan-Shaw S, Nihal M, Ahmad N. Dose translation from animal to human studies revisited. FASEB J 2008; 22:659–61. [PubMed: 17942826]
28. Holick KA, Lee DC, Hen R, Dulawa SC. Behavioral effects of chronic fluoxetine in BALB/cJ mice do not require adult hippocampal neurogenesis or the serotonin 1A receptor. Neuropsychopharmacology 2008; 33:406–17. [PubMed: 17429410]
29. Dulawa SC, Holick KA, Gundersen B, Hen R. Effects of chronic fluoxetine in animal models of anxiety and depression. Neuropsychopharmacology 2004; 29:1321–30. [PubMed: 15085085]
30. Bazhenova EY, Sinyakova NA, Kulikova EA, Iazarinova IA, Bazovkina DV, Gainetdinov RR, et al. No effect of C1473G polymorphism in the tryptophan hydroxylase 2 gene on the response of the brain serotonin system to chronic fluoxetine treatment in mice. Neurosci Lett 2017; 653:264–8. [PubMed: 28579486]
31. Prut L, Belzung C. The open field as a paradigm to measure the effects of drugs on anxiety-like behaviors: a review. Eur J Pharmacol 2003; 463:3–33. [PubMed: 12600700]
32. Slattery DA, Cryan JF. Using the rat forced swim test to assess antidepressant-like activity in rodents. Nature Protoc 2012; 7:1009–14. [PubMed: 22555240]
33. Parihar VK, Limoli CL. Cranial irradiation compromises neuronal architecture in the hippocampus. Proc Natl Acad Sci USA 2013; 110:12822–7. [PubMed: 23858442]
34. Parihar VK, Allen BD, Caressi C, Kwok S, Chu E, Tran KK, et al. Cosmic radiation exposure and persistent cognitive dysfunction. Sci Rep 2016; 6:34774. [PubMed: 27721383]
35. Moser E, Moser MB, Andersen P. Spatial learning impairment parallels the magnitude of dorsal hippocampal lesions, but is hardly present following ventral lesions. J Neurosci 1993; 13:3916–25. [PubMed: 8366351]
36. Bagot RC, Parise EM, Pena CJ, Zhang HX, Maze I, Chaudhury D, et al. Ventral hippocampal afferents to the nucleus accumbens regulate susceptibility to depression. Nat Commun 2015; 6:7062. [PubMed: 25952660]
37. Bannerman DM, Grubb M, Deacon RM, Yee BK, Feldon J, Rawlins JN. Ventral hippocampal lesions affect anxiety but not spatial learning. Behav Brain Res 2003; 139:197–213. [PubMed: 12642189]
38. Kjelstrup KG, Tuvnes FA, Steffenach HA, Murison R, Moser EI, Moser MB. Reduced fear expression after lesions of the ventral hippocampus. Proc Natl Acad Sci U S A 2002; 99:10825–30. [PubMed: 12149439]
39. Parks CL, Robinson PS, Sibille E, Shenk T, Toth M. Increased anxiety of mice lacking the serotonin1A receptor. Proc Natl Acad Sci U S A 1998; 95:10734–9. [PubMed: 9724773]
40. Chalmers DT, Watson SJ. Comparative anatomical distribution of 5-HT1A receptor mRNA and 5-HT1A binding in rat brain-a combined in situ hybridisation/in vitro receptor autoradiographic study. Brain Res 1991; 561:51–60. [PubMed: 1797349]
41. Aznar S, Qian ZX, Shah R, Rahbek B, Knudsen GM. The 5-HT1A serotonin receptor is located on calbindin- and parvalbumin-containing neurons in the rat brain. Brain Res 2003; 959:58–67. [PubMed: 12480158]
42. Albert PR, Lemonde S. 5-HT1A receptors, gene repression, and depression: Guilt by association. Neuroscientist 2004; 10:575–93. [PubMed: 15534042]
43. Stupp R, Dietrich PY, Ostermann Kraljevic S, Pica A, Maillard I, Maeder P, et al. Promising survival for patients with newly diagnosed glioblastoma multiforme treated with concomitant radiation plus temozolomide followed by adjuvant temozolomide. J Clin Oncol 2002; 20:1375–82. [PubMed: 11870182]
44. Wefel JS, Vardy J, Ahles T, Schagen SB. International Cognition and Cancer Task Force recommendations to harmonise studies of cognitive function in patients with cancer. Lancet Oncol 2011; 12:703–8. [PubMed: 21354373]
45. Ahles TA, Saykin AJ. Candidate mechanisms for chemotherapy-induced cognitive changes. Nat Rev Cancer 2007; 7, 192–201. [PubMed: 17318212]

46. Parihar VK, Maroso M, Syage A, Allen BD, Angulo MC, Soltesz I, et al. Persistent nature of alterations in cognition and neuronal circuit excitability after exposure to simulated cosmic radiation in mice. Exp Neurol 2018; 305:44–55. [PubMed: 29540322]
47. Parihar VK, Pasha J, Tran KK, Craver BM, Acharya MM, Limoli CL. Persistent changes in neuronal structure and synaptic plasticity caused by proton irradiation. Brain Struct Funct 2015; 220:1161–71. [PubMed: 24446074]
48. Huang TT, Zou Y, Corniola R. Oxidative stress and adult neurogenesis-effects of radiation and superoxide dismutase deficiency. Semin Cell Dev Biol 2012; 23:738–44. [PubMed: 22521481]
49. Zhao W, Robbins ME. Inflammation and chronic oxidative stress in radiation-induced late normal tissue injury: therapeutic implications. Curr Med Chem 2009; 16:130–43. [PubMed: 19149566]
50. Nokia MS, Anderson ML, Shors TJ. Chemotherapy disrupts learning, neurogenesis and theta activity in the adult brain. Eur J Neurosci 2012; 36:3521–30. [PubMed: 23039863]
51. Yang M, Kim JS, Song MS, Kim SH, Kang SS, Bae CS, et al. Cyclophosphamide impairs hippocampus-dependent learning and memory in adult mice: Possible involvement of hippocampal neurogenesis in chemotherapy-induced memory deficits. Neurobiol Learn Mem 2010; 93:487–94. [PubMed: 20109567]
52. Makale MT, McDonald CR, Hattangadi-Gluth JA, Kesari S. Mechanisms of radiotherapy-associated cognitive disability in patients with brain tumours. Nat Rev Neurol 2017; 13:52–64. [PubMed: 27982041]
53. Janelsins MC, Heckler CE, Thompson BD, Gross RA, Opanashuk LA, Cory-Slechta DA. A clinically relevant dose of cyclophosphamide chemotherapy impairs memory performance on the delayed spatial alternation task that is sustained over time as mice age. Neurotoxicology 2016; 56:287–93. [PubMed: 27371410]
54. Blazquez MH, Cruzado JA. A longitudinal study on anxiety, depressive and adjustment disorder, suicide ideation and symptoms of emotional distress in patients with cancer undergoing radiotherapy. J Psychosom Res 2016; 87:14–21. [PubMed: 27411747]
55. Cardoso G, Graca J, Klut C, Trancas B, Papoila A. Depression and anxiety symptoms following cancer diagnosis: a cross-sectional study. Psychol Health Med 2016; 21:562–70. [PubMed: 26683266]
56. Mehnert A, Lehmann C, Graefen M, Huland H, Koch U. Depression, anxiety, post-traumatic stress disorder and health-related quality of life and its association with social support in ambulatory prostate cancer patients. Eur J Cancer Care (Engl) 2010; 19:736–45. [PubMed: 19832893]
57. Merikangas KR, Zhang HP, Avenevoli S, Acharyya S, Neuenschwander M, Angst J. Longitudinal trajectories of depression and anxiety in a prospective community study - The Zurich cohort study. Arch Gen Psychiat 2003; 60:993–1000. [PubMed: 14557144]
58. Cryan JF, Holmes A. The ascent of mouse: advances in modelling human depression and anxiety. Nat Rev Drug Discov 2005; 4:775–90. [PubMed: 16138108]
59. Anderson VA, Godber T, Smibert E, Weiskop S, Ekert H. Cognitive and academic outcome following cranial irradiation and chemotherapy in children: a longitudinal study. Br J Cancer 2000; 82:255–62. [PubMed: 10646874]
60. Albert PR, Francois BL. Modifying 5-HT1A receptor gene expression as a new target for antidepressant therapy. Front Neurosci 2010; 4:35. [PubMed: 20661455]
61. Millan MJ. The role of monoamines in the actions of established and “novel” antidepressant agents: a critical review. Eur J Pharmacol 2004; 500:371–84. [PubMed: 15464046]
62. Jans LA, Riedel WJ, Markus CR, Blokland A. Serotonergic vulnerability and depression: assumptions, experimental evidence and implications. Mol Psychiatry 2007; 12:522–43. [PubMed: 17160067]
63. aan het Rot M 63, Mathew SJ, Charney DS. Neurobiological mechanisms in major depressive disorder. CMAJ 2009; 180:305–13. [PubMed: 19188629]
64. Toth M 5-HT1A receptor knockout mouse as a genetic model of anxiety. Eur J Pharmacol 2003; 463:177–84. [PubMed: 12600709]
65. Kreisman NR, Soliman S, Gozal D. Regional differences in hypoxic depolarization and swelling in hippocampal slices. J Neurophysiol 2000; 83:1031–8. [PubMed: 10669514]

66. Verge D, Daval G, Marcinkiewicz M, Patey A, Elmestikawy S, Gozlan H, et al. Quantitative autoradiography of multiple 5-Ht1 receptor subtypes in the brain of control or 5,7-dihydroxytryptamine-treated rats. J Neurosci 1986; 6:3474–82. [PubMed: 2947981]

67. Kia HK, Miquel MC, Brisorgueil MJ, Daval G, Riad M, El Mestikawy S, et al. Immunocytochemical localization of serotonin 1A receptors in the rat central nervous system. J Comp Neurol 1996; 365:289–305. [PubMed: 8822171]

68. Gozal E, Gozal D, Pierce WM, Thongboonkerd V, Scherzer JA, Sachleben LR, Jr., et al. Proteomic analysis of CA1 and CA3 regions of rat hippocampus and differential susceptibility to intermittent hypoxia. J Neurochem 2002; 83:331–45. [PubMed: 12423243]

69. Wang XK, Pal R, Chen XW, Limpeanchob N, Kumar KN, Michaelis EK. High intrinsic oxidative stress may underlie selective vulnerability of the hippocampal CA1 region. Mol Brain Res 2005; 140:120–6. [PubMed: 16137784]

70. Schmidt-Kastner R, Freund TF. Selective vulnerability of the hippocampus in brain ischemia. Neuroscience 1991; 40:599–636. [PubMed: 1676492]

71. Riley PA. Free radicals in biology: oxidative stress and the effects of ionizing radiation. Int J Radiat Biol 1994; 65:27–33. [PubMed: 7905906]

72. Azzam EI, Jay-Gerin JP, Pain D. Ionizing radiation-induced metabolic oxidative stress and prolonged cell injury. Cancer Lett 2012; 327:48–60. [PubMed: 22182453]

73. Joshi G, Sultana R, Tangpong J, Cole MP, St Clair DK, Vore M, et al. Free radical mediated oxidative stress and toxic side effects in brain induced by the anti cancer drug adriamycin: Insight into chemobrain. Free Radical Res 2005; 39:1147–54. [PubMed: 16298740]

74. Tseng BP, Giedzinski E, Izadi A, Suarez T, Lan ML, Tran KK, et al. Functional consequences of radiation-induced oxidative stress in cultured neural stem cells and the brain exposed to charged particle irradiation. Antioxid Redox Signal 2014; 20:1410–22. [PubMed: 23802883]

75. Andrade R Regulation of membrane excitability in the central nervous system by serotonin receptor subtypes. Ann N Y Acad Sci 1998; 861:190–203. [PubMed: 9928257]

76. Andrade R, Nicoll RA. Pharmacologically distinct actions of serotonin on single pyramidal neurones of the rat hippocampus recorded in vitro. J Physiol 1987; 394:99–124. [PubMed: 3443977]

77. Schmitz D, Empson RM, Heinemann U. Serotonin reduces inhibition via 5-HT1A receptors in area CA1 of rat hippocampal slices in vitro. J Neurosci 1995; 15:7217–25. [PubMed: 7472476]

78. Beck SG. 5-Hydroxytryptamine increases excitability of CA1 hippocampal pyramidal cells. Synapse 1992; 10:334–40. [PubMed: 1585262]

79. Fenn AM, Gensel JC, Huang Y, Popovich PG, Lifshitz J, Godbout JP. Immune activation promotes depression 1 month after diffuse brain injury: A role for primed microglia. Biol Psychiat 2014; 76:575–84. [PubMed: 24289885]

80. Robbins ME, Zhao W. Chronic oxidative stress and radiation-induced late normal tissue injury: a review. Int J Radiat Biol 2004; 80:251–9. [PubMed: 15204702]

81. Suman S, Rodriguez OC, Winters TA, Fornace AJ Jr., Albanese C, Datta K. Therapeutic and space radiation exposure of mouse brain causes impaired DNA repair response and premature senescence by chronic oxidant production. Aging (Albany NY) 2013; 5:607–22. [PubMed: 23928451]

82. Cakmak G, Miller LM, Zorlu F, Severcan F. Amifostine, a radioprotectant agent, protects rat brain tissue lipids against ionizing radiation induced damage: An FTIR microspectroscopic imaging study. Arch Biochem Biophys 2012; 520:67–73. [PubMed: 22402174]

83. Hong JH, Chiang CS, Campbell IL, Sun JR, Withers HR, Mcbride WH. Induction of acute-phase gene-expression by brain irradiation. Int J Radiat Oncol 1995; 33:619–26.

84. Kettenmann H, Hanisch UK, Noda M, Verkhratsky A. Physiology of microglia. Physiol Rev 2011; 91:461–553. [PubMed: 21527731]

85. Kreutzberg GW. Microglia: a sensor for pathological events in the CNS. Trends Neurosci 1996; 19:312–8. [PubMed: 8843599]

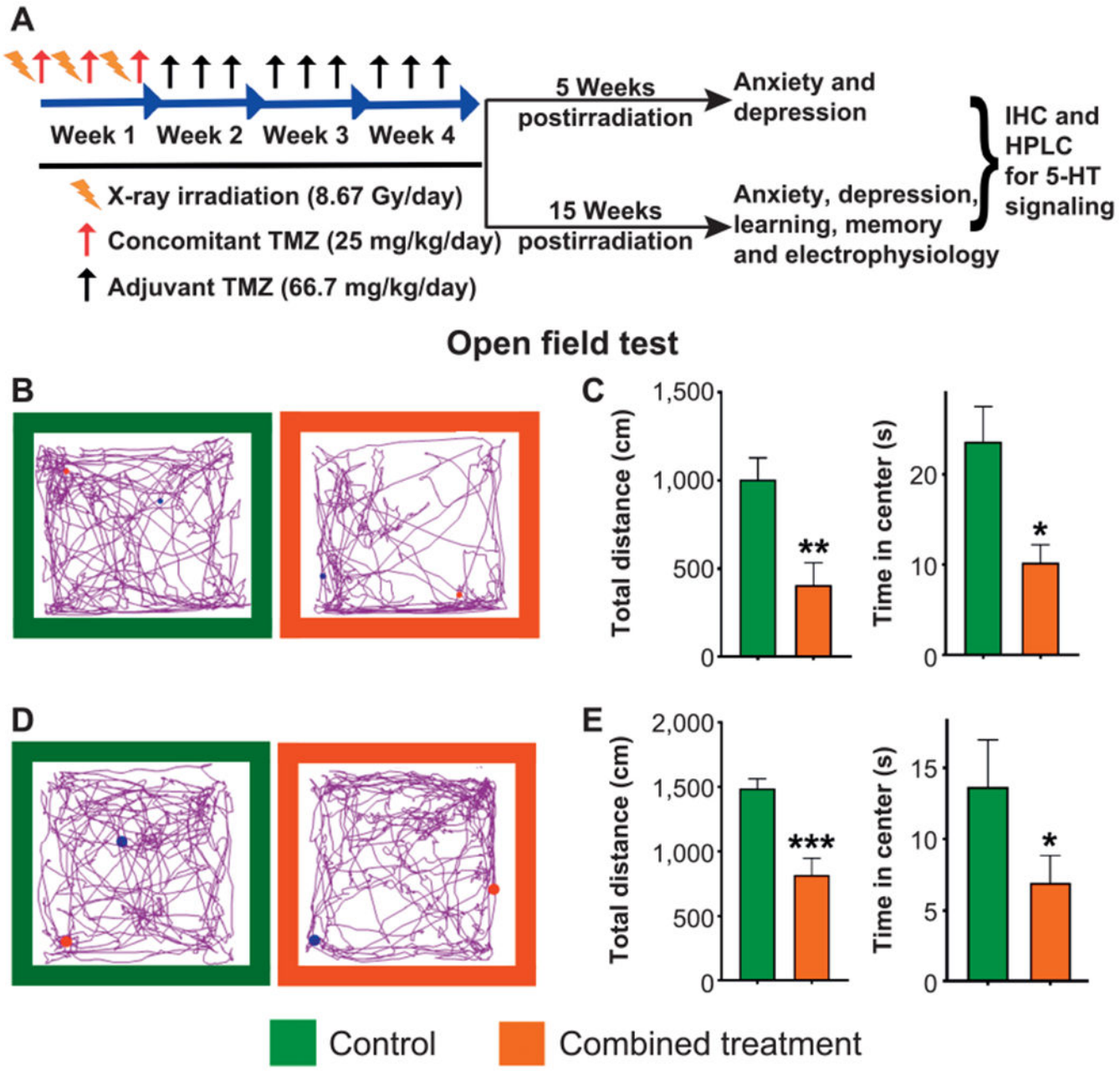

FIG. 1.

Combined treatment promotes anxiety-like tendencies in an open field. Panel A: Experimental design. Six-month-old male C57BL/6J mice received three X-ray doses of 8.67 Gy in week 1 interspersed with concomitant doses of TMZ administered intraperitoneally (i.p., 25 mg/kg). Mice then received nine adjuvant doses (66.7 mg/kg) of TMZ (i.p.) in the subsequent 3 weeks (3 alternating days/week). The first cohort of mice was subjected to behavioral testing at 5 weeks postirradiation and the second at 15 weeks postirradiation followed by immunohistochemistry and HPLC studies for both cohorts and electrophysiology for the 15-week cohort. These time points were specifically counted from the final day of irradiation. Panel B: Representative movement tracking of control and

combined treatment mice in the 5-min open field test at 5 weeks postirradiation. Panel C: Combined treatment mice traveled significantly less distance than control mice (408 ± 123 cm and 1,004 ± 120 cm, respectively) and spent significantly less time in the central zone compared to the control animals (10.2 ± 2.0 s and 23.6 ± 4.0 s, respectively). Panel D: Representative movement tracking of control and combined treatment mice in the 5-min open field test at 15 weeks postirradiation. Panel E: Combined treatment mice travelled significantly less distance than control mice (817 ± 130 cm and 1,487 ± 80 cm, respectively) and spent significantly less time in the central zone compared to the control animals (6.9 ± 2.0 s and 13.6 ± 3.0 s, respectively). For the 5-week cohorts, n = 10 for the control and n = 9 for the combined treatment group. For the 15-week cohorts, n = 15 for the control and n = 14 for the combined treatment group. Data are presented as mean ± SEM. *P* values are derived using the Mann-Whitney U test. $*P < 0.05$, $**P < 0.01$, $***P < 0.001$.

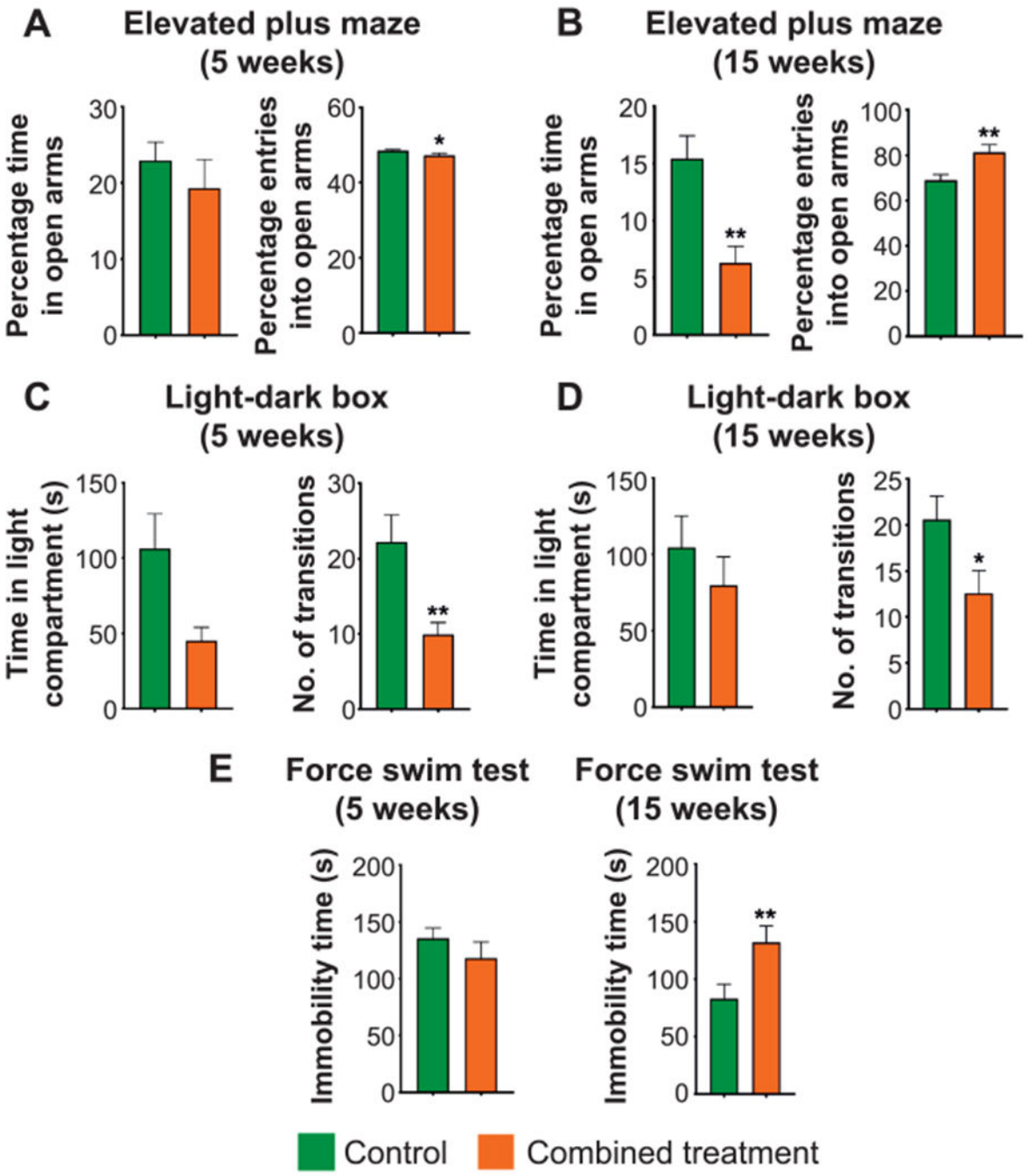

FIG. 2.

Combined treatment induces anxiety- and depression-like behavior. Panel A: At 5 weeks postirradiation combined treatment mice spent a similar percentage of time in the open arms of the EPM compared to the control mice (19.3 ± 3.8 and 23 ± 2.0, respectively), but differed significantly in the percentage of entries into the open arms (47 ± 0.6 and 49 ± 0.2, respectively). Panel B: At 15 weeks postirradiation, the percentage of time spent in the open arms of the EPM by combined treatment mice was less than that of control mice (6.3 ± 1.5 and 15.4 ± 2.0, respectively), but combined treatment mice made more entries into the open

arms compared to controls (81.2 ± 4.0 and 68.6 ± 2.8, respectively). Panel C: At 5 weeks postirradiation no significant difference in the time spent in the light compartment of the light-dark box arena was found between combined treatment and control mice (45.2 ± 8.7 and 106.3 ± 23.1, respectively). However, combined treatment mice had fewer numbers of transitions between compartments compared to controls (10 ± 2.0 and 22 ± 4.0, respectively). Panel D: At 15 weeks postirradiation, combined treatment and control mice spent similar times in the light compartment of the light-dark box (79.7 ± 18.7 and 104.4 ± 20.5, respectively). However, combined treatment mice had fewer numbers of transitions between compartments compared to controls (13 ± 2.0 and 21 ± 3.0, respectively). Panel E: At 5 weeks postirradiation on the forced swim test the combined treatment and control mice spent similar amounts of time floating (118.2 ± 14.0 s and 135.7 ± 9.0 s, respectively), but at the late time point the combined treatment mice spent significantly more time floating than did the controls (132 ± 14.1 s and 83 ± 12.7 s, respectively). For the EPM and LDB 5-week cohorts, n = 10 for the control group and n = 9 for the combined treatment group; for the 15-week cohort, n = 15 for the control group and n = 14 for the combined treatment group. For the FST 5-week cohorts, n = 9 each for the control and combined treatment groups; and for the 15-week cohort, n = 6 each for the control and combined treatment groups. Data are presented as mean ± SEM. P values are derived from the Mann-Whitney U test. $*P < 0.05$, $**P < 0.01$.

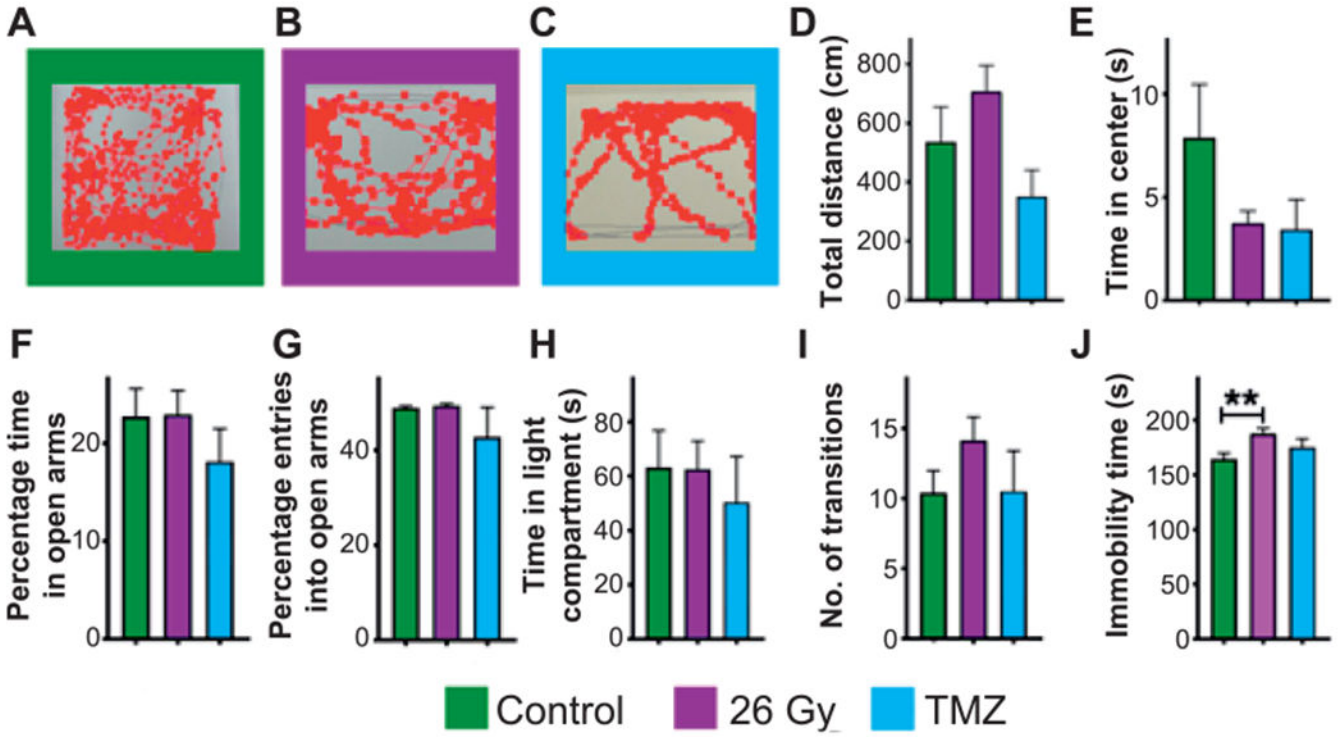

FIG. 3.

Individual treatment with radiation or TMZ does not cause anxiety. Panels A–C: Representative movement tracking of 0 Gy (control), 26 Gy (radiation alone) and TMZ-only treated mice, respectively, in the 5min open field test. Panel D: No significant difference in distance travelled was observed in individually treated groups of mice (536 ± 120 cm, 707 ± 88 cm and 351 ± 90 cm, for control, 26 Gy and TMZ, respectively). Panel E: Similarly, no significant difference in time spent in the center zone was observed in individually treated groups of mice (7.8 ± 2.6 s, 3.7 ± 0.6 s and 3.4 ± 1.4, for control, 26 Gy and TMZ, respectively). Panel F: The EPM test also revealed no significant difference in the percentage of time spent in open arms of the maze between the three groups (23 ± 3, 23 ± 3 and 18 ± 3 for control, 26 Gy and TMZ, respectively); and (panel G) the number of the entries into the open arms was also similar among all groups (49 ± 0.3, 49 ± 0.4 and 43 ± 6 for control, 26 Gy and TMZ, respectively). Panel H: LDB testing similarly showed no differences in the time spent in the light compartment among groups (63 ± 14, 62 ± 10 and 74 ± 26 for control, 26 Gy and TMZ, respectively) and (panel I) no difference in the number of transitions (10 ± 2, 14 ± 2 and 11 ± 3 for control, 26 Gy and TMZ, respectively). Panel J: In the FST, the irradiated mice exhibited more time floating than either control or TMZ-treated mice (165 ± 5, 188 ± 5 and 175 ± 8 for control, 26 Gy and TMZ, respectively). For these studies, the control n = 12 for all tasks; the 26 Gy cohort n = 14 for panels A–I and n = 13 for panel J; and the TMZ cohort n = 7 for panels A–G, n = 6 for panels H–I and n = 5 for panel J. Data are presented as mean ± SEM. *P* values are derived from one-way ANOVA. $^{**}P < 0.01$

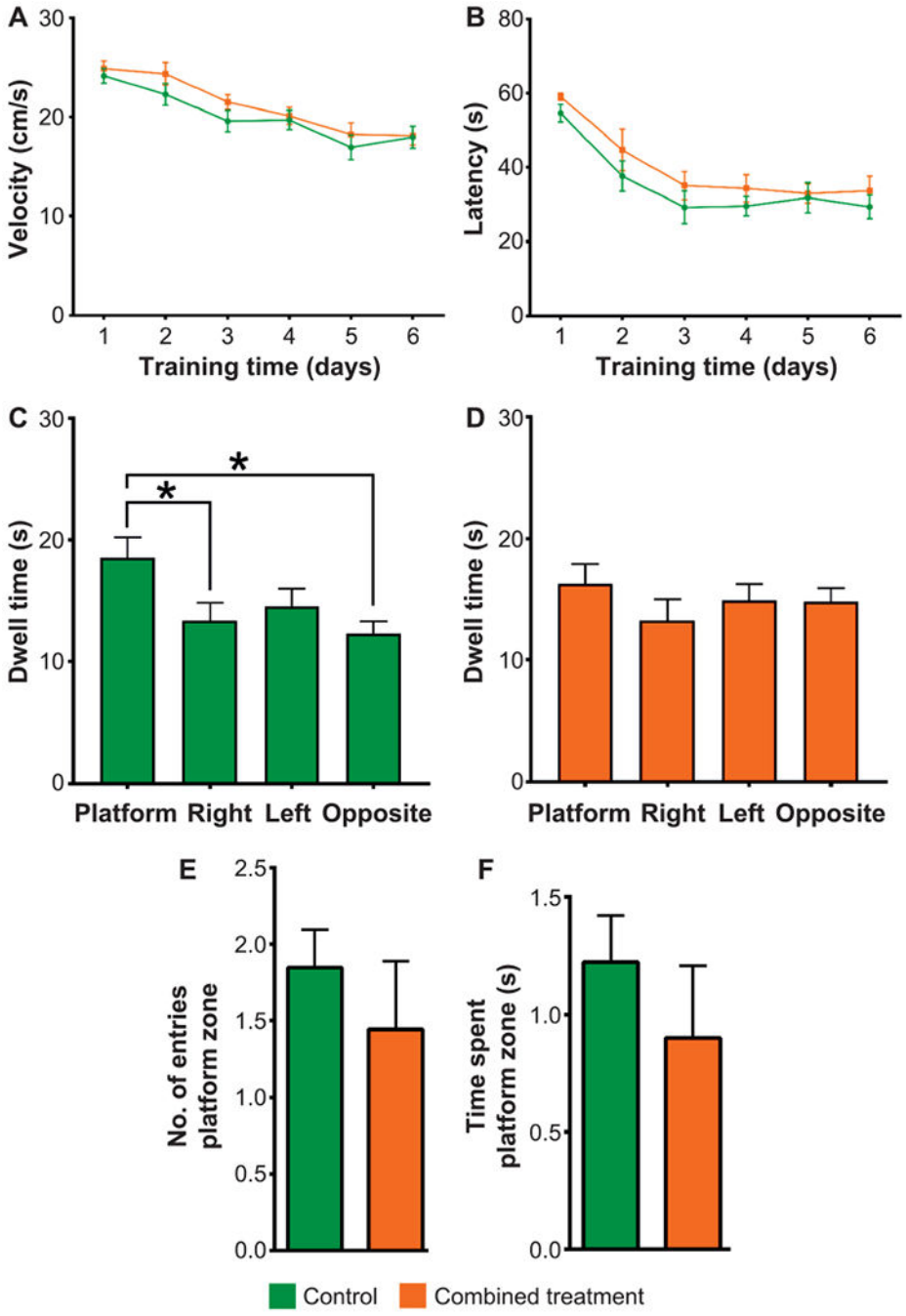

FIG. 4.

Effects of combined treatment on cognitive impairments using the MWM at 15 weeks postirradiation. Panel A: The swimming velocity (cm/s) was similar between control and combined treatment mice; and (panel B) no change was found in learning between the combined treatment and control mice, as measured by latency to locate the platform. Panel C: As measured by dwell time, control mice exhibited a clear preference for the original platform quadrant, which was greater than the time spent in the right and opposite quadrant during the memory retrieval test (right 13.3 ± 1.5 s; opposite 12.3 ± 0.9 s; left 14.5 ± 1.4 s;

platform 18.5 ± 1.7 s); however, (panel D), combined treatment mice exhibited no quadrant preference during the memory retrieval task (right 13.3 ± 1.8 s; opposite 14.8 ± 1.1 s; left 14.9 ± 1.3 s, platform 16.3 ± 1.7 s). Control n = 13 and combined treatment n = 9. Data are presented as mean ± SEM. *P* values are derived from (panels A and B) two-way RM ANOVA with Bonferonni's multiple comparisons. Panels C and D: Paired Student's *t* test was used; $*P < 0.05$. Panels E and F: Wilcoxon matched-pairs signed rank test was used.

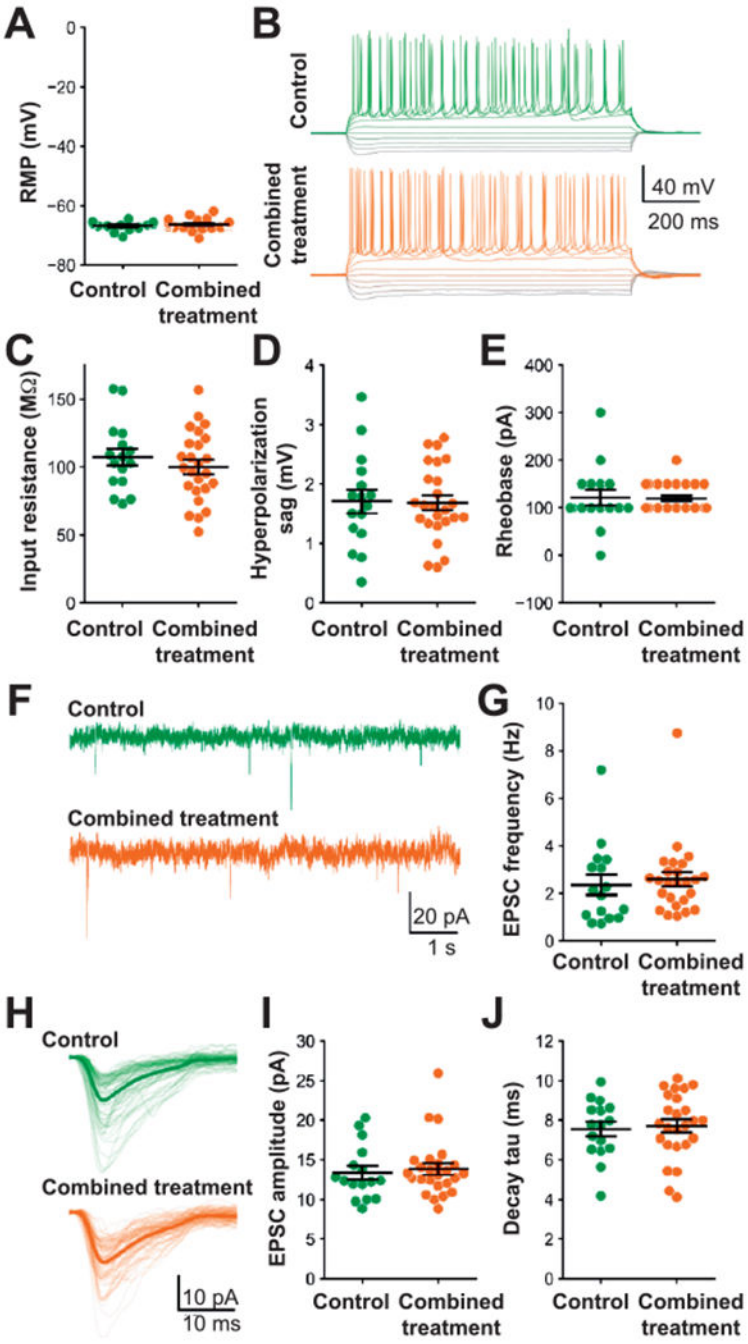

FIG. 5.

Electrophysiological properties of CA1 pyramidal neurons are not altered after combined treatment. All data are from whole-cell recordings of CA1 pyramidal neurons from the superficial layer of the ventral hippocampus. Panel A: Resting membrane potential was unchanged between combined treatment and control mice. Panel B: Representative examples of responses to a range of brief current injections in control and combined treatment neurons. There was no alteration in the (panel C) input resistance, (panel D) sag during a −100 pA hyperpolarizing current injection, (panel E) or rheobase current required to evoke

an action potential between the treatment groups. Panel F: Representative examples of recordings containing spontaneous EPSCs from control and combined treatment neurons. Panel G: The frequency of sEPSCs was equivalent between control and combined treatment neurons. Panel H: Examples of EPSCs in representative control and combined treatmnet neurons. Light lines show individual sEPSCs, while the darker line displays the average sEPSC during a 200-s recording from that neuron. Neither (panel I) sEPSC amplitude nor (panel J) the sEPSC decay time-constant was shifted between groups. Control n = 16 cells and combined treatment n = 25 cells for all plots showing grouped data.

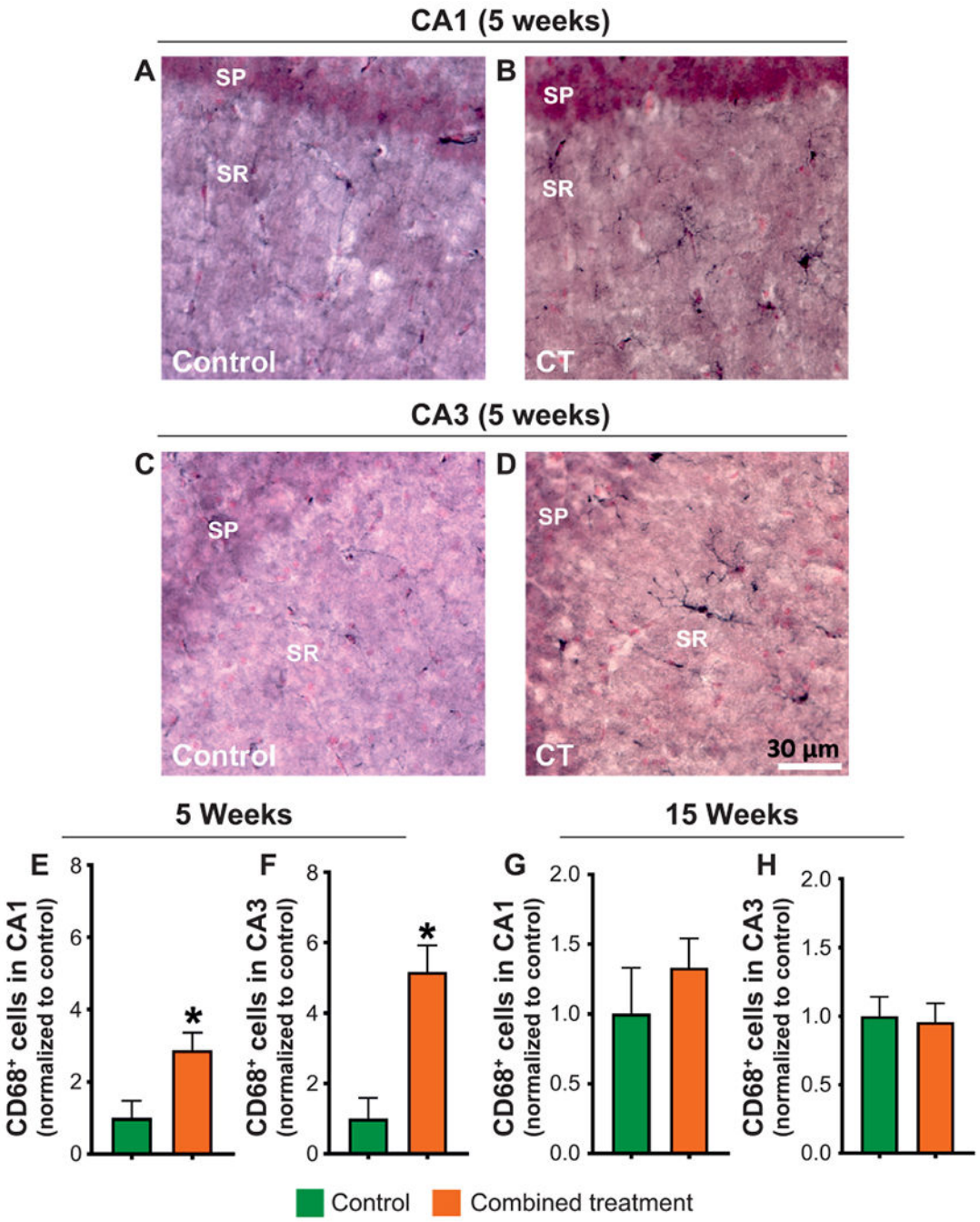

FIG. 6.

Microglial activation is acutely elevated by combined treatment. Representative images of $CD68^+$ activated microglia immunohistochemistry in the CA1 (panels A and B) and CA3 (panels C and D) regions of the hippocampus of control and combined treatment mice at 5 weeks postirradiation. CT = combined treatment. Panel E: Increased numbers of activated microglia were found at 5 weeks postirradiation in the CA1 region of the hippocampus of combined treatment mice compared to controls (4854 ± 413 control and 1690 ± 407 combined treatment, $CD68^+$ cells) and (panel F) in the CA3 region of combined treatment

mice compared to controls (3526 ± 254 control and 681.8 ± 199 combined treatment, $CD68^+$ cells). Relative to controls, no change in microglial activation was observed at 15 weeks postirradiation in either the CA1 (panel G; 20,060 ± 197 control and 22,050 ± 274 combined treatment, $CD68^+$ cells) or CA3 (panel H) region of the hippocampus (16,540 ± 411 control and 15,770 ± 167 combined treatment, $CD68^+$ cells). Black indicates the $CD68^+$ cells and red indicates the nuclear fast red counterstain; Scale bar = 30 μm. The number of $CD68^+$ cells in each combined treatment group is normalized to the number of $CD68^+$ cells in the control group and presented as mean ± SEM for n = 4 mice/group. *P* values are derived from the Mann-Whitney U test. $*P < 0.05$.

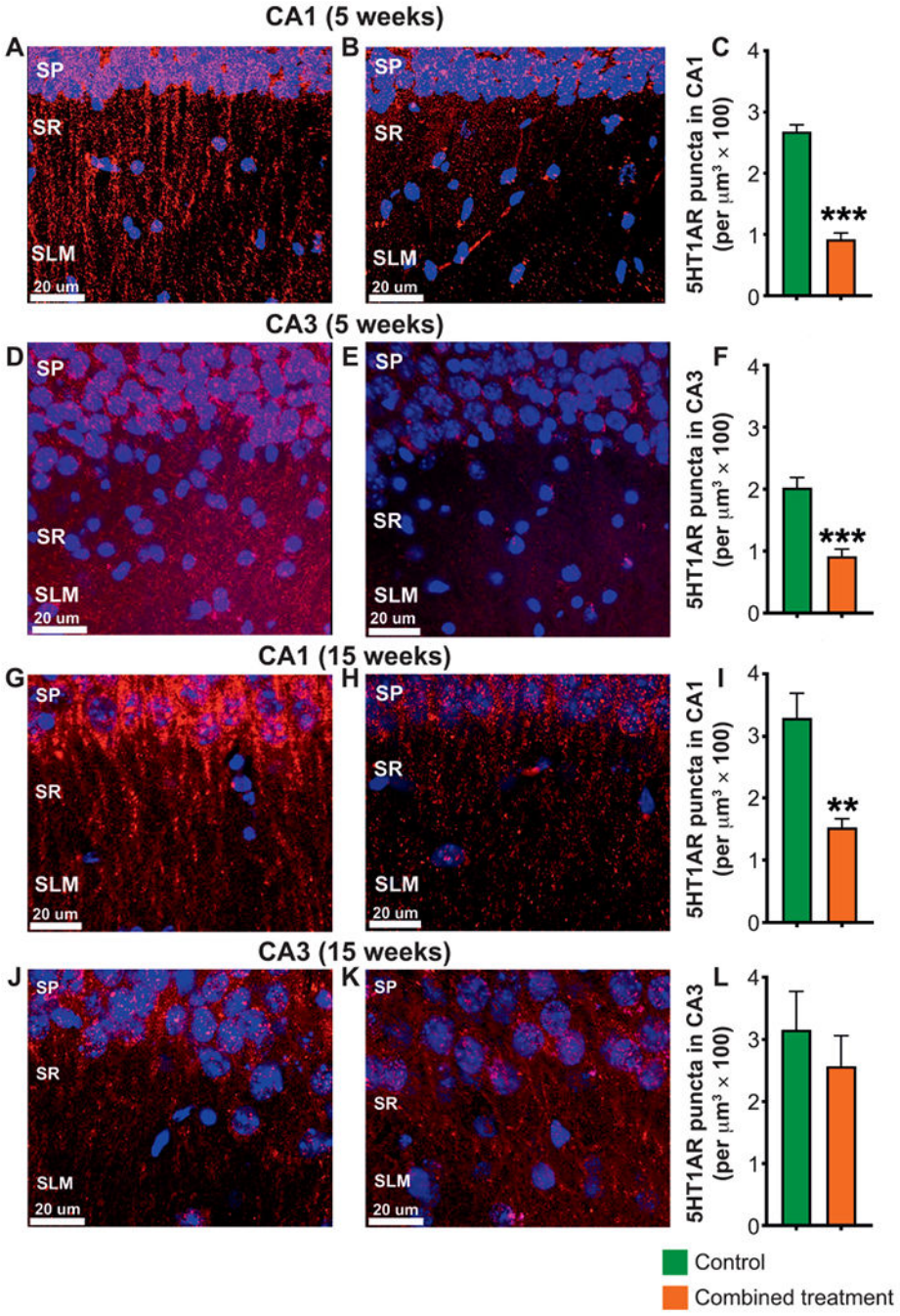

FIG. 7.

Combined treatment alters hippocampal serotonin receptor 5HT1A receptor (5HT1AR) levels. Panels A and B: Representative images of 5HT1AR immunohistochemistry in the CA1 region of the hippocampus in control and combined treatment mice at 5 weeks postirradiation, respectively. Panel C: Combined treatment mice had reduced numbers of 5HT1AR puncta per $\mu m^3 \times 100$ in the CA1 region of the hippocampus compared to control mice at 5 weeks postirradiation (0.92 ± 0.1 and 2.7 ± 0.1, respectively). Panels D and E: Representative images of 5HT1A receptor immunohistochemistry in the CA3 region of the

hippocampus in control and combined treatment mice at 5 weeks postirradiation, respectively. Panel F: At 5 weeks postirradiation, fewer 5HT1AR puncta were also observed in the CA3 region of the hippocampus of combined treatment compared to control mice (0.92 ± 0.1 and 2.02 ± 0.2, respectively). Panels G and H: Representative images of 5HT1A receptor immunohistochemistry in the CA1 region of the hippocampus in control and combined treatment mice at 15 weeks postirradiation, respectively, at which time (panel I), combined treatment mice had reduced numbers of 5HT1AR puncta in the CA1 region of the hippocampus compared to control mice (1.5 ± 0.1 and 3.3 ± 0.4, respectively). Panels J and K: Representative images of 5HT1A receptor immunohistochemistry in the CA3 region of the hippocampus in control and combined treatment mice, respectively, at 15 weeks postirradiation, at which time (panel L) levels of 5HT1AR in the CA3 region of the hippocampus of combined treatment mice were indistinguishable from that of controls (2.5 ± 0.4 and 3.2 ± 0.6, respectively). Red indicates 5HT1AR; blue indicates DAPI counterstain. Scale bar = 20 μm. SP = stratum pyramidale, SR = stratum radiatum and SLM = stratum lacunosum moleculare. Data are presented as mean ± SEM for n = 4 mice/group. *P* values are derived using Mann-Whitney U test. $^{**}P < 0.01$, $^{***}P < 0.001$.

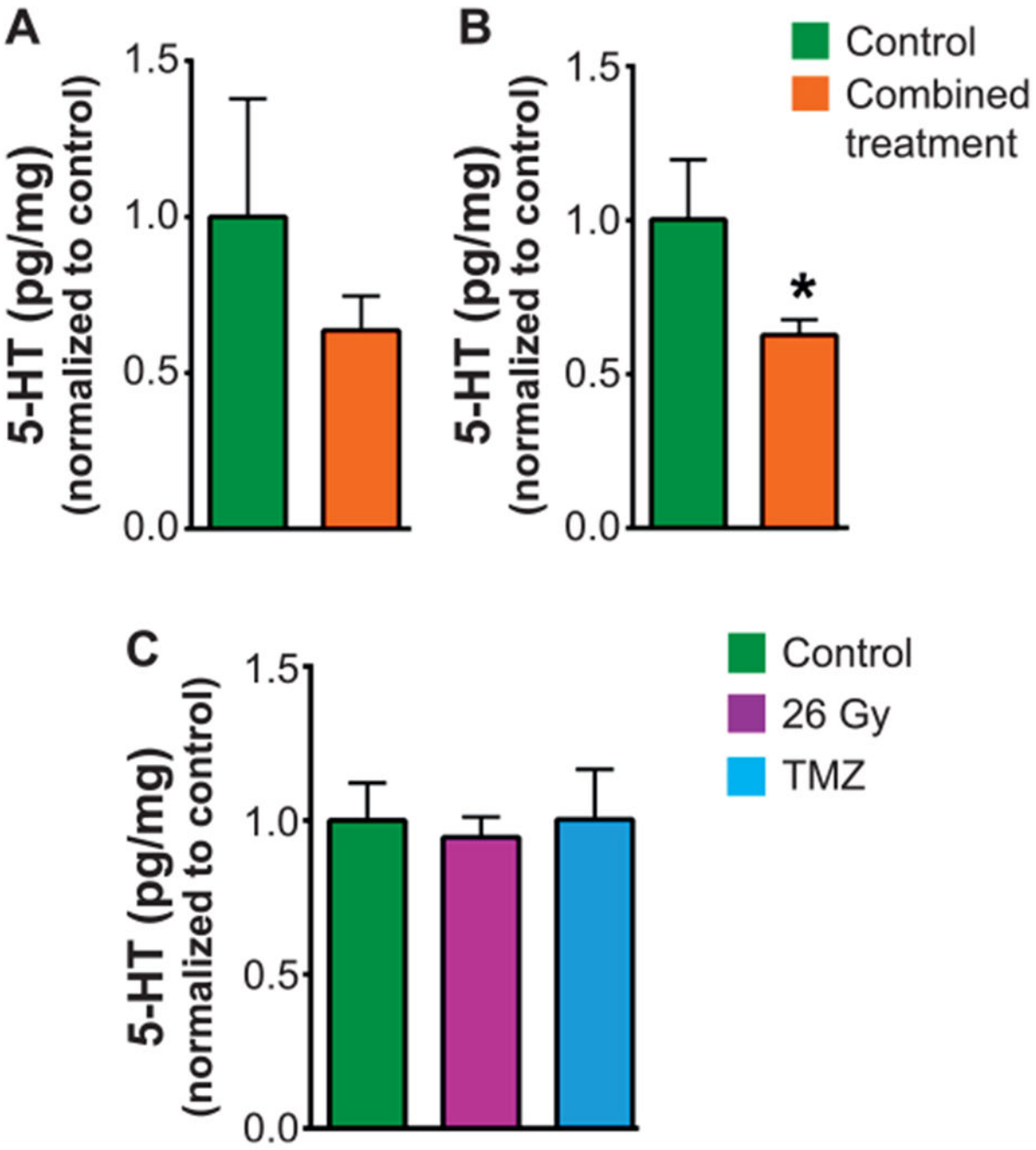

FIG. 8.

Hippocampal serotonin levels are reduced after combined treatment, but not after individual therapies. Panel A: The levels of 5-HT were similar in combined treatment and control mice at 5 weeks postirradiation. Panel B: However, at 15 weeks postirradiation combined treatment mice had lower levels of 5-HT compared to controls. Panel C: Compared to controls, mice treated with radiation alone (26 Gy) or with TMZ alone showed no evidence of decreased hippocampal levels of 5-HT at 15 weeks postirradiation. Levels of 5-HT are normalized to that of the control. For the combined treatment study, data are presented as

mean ± SEM, n = 6–8 mice/group, and *P* values are derived using Mann-Whitney U test. **P* < 0.05. For the individual therapy study, data are presented as mean ± SEM n = 4–6 mice/group and *P* values are derived using one-way ANOVA.

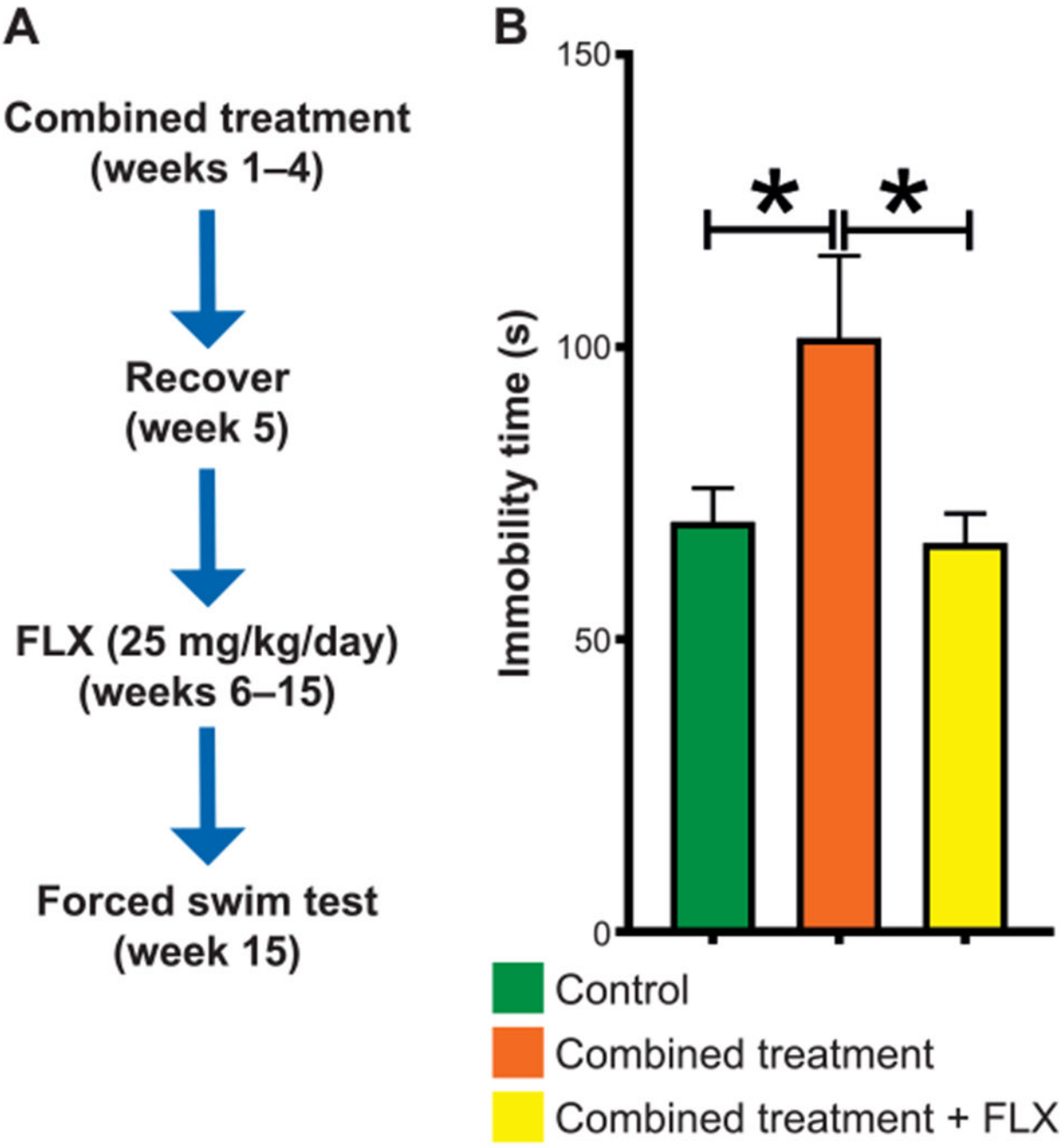

FIG. 9.

Fluoxetine alleviates combined treatment-induced depression-like behavior. Panel A: Six-month-old male mice received combined treatment and were then allowed to recover for one week before beginning fluoxetine (FLX) treatment (25 mg/kg/day). Mice remained on FLX until 15 weeks postirradiation at which time FST was conducted. Panel B: Mice receiving combined treatment with FLX spent significantly less time floating than mice given combined treatment alone (66.5 ± 5.1 s and 101.5 ± 14.0 s, respectively). Similarly, combined treatment mice spent significantly more time floating than controls (101.5 ± 14.0 s

and 70.0 ± 5.8 s, respectively). No difference in floating time was found between control mice and those receiving combined treatment with FLX ($P = 0.8$). For these studies, n = 8 for the controls, n = 7 for the combined treatment group and n = 6 for the combined treatment with FLX group. Data are presented as mean ± SEM. P values are derived using one-way ANOVA. *$P < 0.05$.